AD-A058 527 ROCHESTER UNIV N Y INST OF OPTICS F/G 11/3
OPTICAL INTERFERENCE COATINGS FOR THE ULTRAVIOLET.(U)
JUL 78 P W BAUMEISTER N00014-77-C-0573
UNCLASSIFIED NL

END
DATE FILMED
11-78
DDC

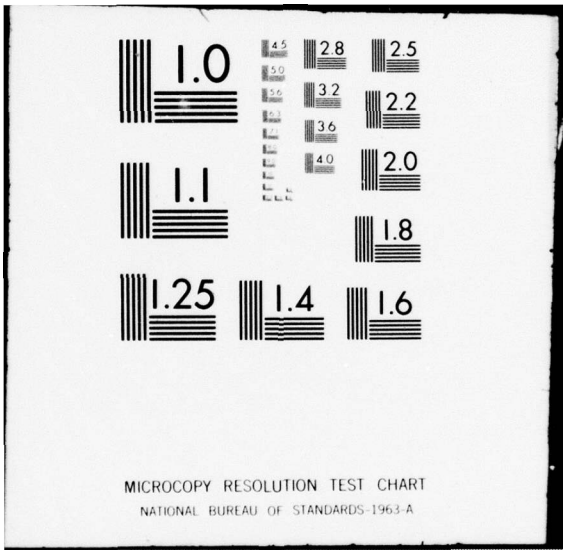
1.0
1.1
1.25
1.4
1.6
1.8
2.0
2.2
2.5
2.8
3.2
3.6
4.0
4.5
5.0
5.6
6.3
MICROCOPY RESOLUTION TEST CHART
NATIONAL BUREAU OF STANDARDS-1963-A

THE UNIVERSITY OF ROCHESTER
THE INSTITUTE OF OPTICS
ROCHESTER, NEW YORK

LEVEL

12 NW

Optical Interference Coatings for the Ultraviolet

Final Progress Report

covering the period

August 1, 1977 to July 31, 1978

Research Contract N00014-77-C-0573

Office of Naval Research

1030 East Green Street

Pasadena, California 91106

Principal Investigator:

Philip Baumeister

(6) Optical Interference Coatings for the Ultraviolet.

(9) Final ~~Progress~~ Report. 1 Aug 77-31 Jul 78,
covering the period

August 1, 1977 to July 31, 1978

(15) Research Contract N00014-77-C-0573 new

with

(11) 31 Jul 78

Office of Naval Research
1030 East Green Street
Pasadena, California 91106

(12) 56 p.

under the auspices of
Naval Weapons Center
Michelson Laboratory
China Lake, California
Principal Investigator: P.W. Baumeister

The Institute of Optics
University of Rochester
Rochester, New York 14627

(19) Philip W. Baumeister

A B S T R A C T

All dielectric multilayer reflectors were constructed with a radiant reflectance R in excess of 99% at a wavelength of 250 nm. The stacks contained the following materials: hafnia, silica, magnesium fluoride, and yttria.

Reflectors were also prepared using alternate layers of silica and hafnia. A maximum reflectance in excess of 0.995 was obtained at 355 nm.

Spectroreflectometry was used to determine the refractive index versus wavelength of the following optical coating materials: hafnia, yttria, lanthanum sesquioxide, and tantalum pentoxide. All of these materials, with the exception of the latter, are optically transparent to wavelengths as short as 250 nm.

Table of contents

II. Experimental procedures

2.1 Introduction

Our objective was to deposit multilayer reflectors for the ultraviolet region by vacuum evaporation. An existing evaporation tank was refitted and re-instrumented as follows: (1) Re-installation of the ultraviolet optical monitoring system; and (2) Installation of improved substrate heaters and temperature control.

2.2 Description of coating apparatus

The UV coatings are deposited in a vacuum tank that is 0.76 m in diameter by 1.52 m in height.

Figure 1 shows the coating chamber and associated optical monitoring system. The hydrogen lamp H is imaged by quartz lenses L on the slit of the grating monochromator G. The flux is directed through a mechanical chopper C, through the window W into the tank and thence upon the rotary holder that positions a quartz monitoring plate P in the beam. The reflected flux is then directed towards the exit window W and the monochromator. The only precaution is to insert an absorbing filter (Schott UG series) to reduce the scattered flux in the grating monochromator. The selection of the wavelength for optical monitoring is discussed below. The electrical signal from a 1P-28 photomultiplier (detector D) is fed into an amplifier and thence into a strip chart recorder.

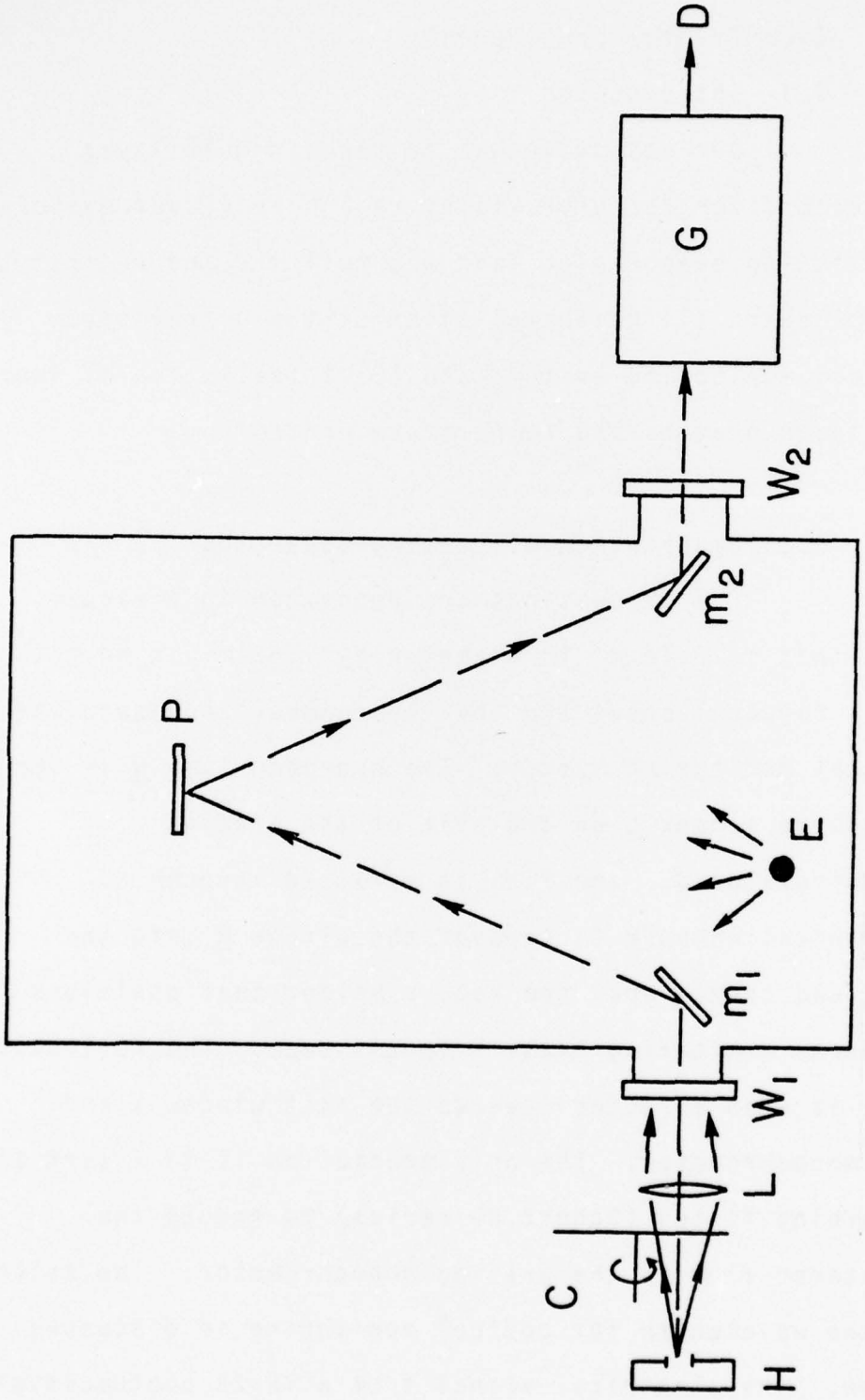

Fig. 1

The evaporator used for the deposition of thin layers.

Elstein type radiation heaters were installed to heat the substrates during deposition. The heaters were positioned at a distance of approximately 15 cm from the substrates. The Elstein heaters have the advantage that they operate at a relatively low temperature and hence a substantial part of the radiation is absorbed by the silica substrates. The temperature is monitored with a thermocouple that is enclosed in a glass tube so that the transfer of radiant energy approximates that of the substrate.

2.3 Optical monitoring

The optical thicknesses of the layers were monitored optically by halting the deposition when the radiant reflectance reached a maximum or minimum. This produces quarterwave optical thickness layers.

Because of the nonnormal incidence of the flux upon the monitoring plate, the wavelength of the monochromator must be set at a wavelength that is about 7.5% shorter than the wavelength where a quarterwave optical thickness is desired. For example, if a film with a quarterwave optical thickness at 355 nm is desired, the monochromator is set at 324 nm. This posed no problems at 355 nm. But when the layers were deposited at the shorter wavelength of 250 nm, electrical signals from the 1P-28 dropped to low enough levels that the noise hindered the accurate

measurement of the maxima and minima of the reflectance versus time. This was solved by monitoring at a longer wavelength and using a rotating sector, as described below.

Three substrates were held in a jig that was rotated during deposition. A wedged-shaped mask was positioned underneath which covered the substrates during a fraction of each revolution. The effect was to produce a coating on the substrates that was thinner than the optical monitor plates. All of the mirrors at 250 nm were coated by this technique.

2.4 Optical coating materials and deposition

The following optical coating materials were considered for the dielectric mirrors:

OXIDES	FLUORIDES
aluminum oxide	ceric fluoride
hafnium dioxide	lanthanum fluoride
lanthanum oxide	magnesium fluoride
scandium oxide	
silica	
tantalum pentoxide	
thorium dioxide	
yttrium oxide	
zirconium dioxide	

Most of the foregoing materials are relatively transparent at 350 nm -- with the possible exception of tantalum pentoxide. Yttria and lanthanum oxide have relatively lower refractive indices and consequently more layers are needed to produce a given reflectance, as compared to the other materials.

Thoria is refractory in the extreme and difficult to evaporate, as well as being slightly radioactive. Since we have more experience in depositing layers of HfO_2, we decided to use HfO_2 and SiO_2 as the high and low index materials in the multilayer reflectors [1].

The former material was prepared for vacuum evaporation by the Merck Company. The hot-pressed tablets of HfO_2 were deposited with the electron gun at 1.1 KW power. The deposition of the granules of SiO_2 required only one-quarter of that power. The base pressure in the chamber was reduced to less $5\ 10^{-6}$ torr before evaporation. Oxygen was re-addmitted to raise the pressure to $5\ 10^{-5}$ torr. This assisted in oxydizing the evaporants more fully.

The fused silica, SiC, or Mo substrates were heated with the radiant heaters described earlier. The heat transfer from the heaters to the substrates is via radiant flux, principally in the infrared. An indication of the substrate temperature is obtained from a thermocouple that is encased in a glass tube. Since the infrared absorption of glass and the fused silica are very nearly the same, the thermocouple temperature is close to that of the bulk temperature of the fused silica. The surface

temperature of the fused silica, however, may be considerably higher than the bulk, due to the heat of sublimation of the evaporant. A temperature in the range 200°C to 250°C was used in all of the evaporations. The higher temperature is needed to oxydize the evaporants. The Mo substrates, on the other hand, absorb considerably less flux from the heaters and were undoubtedly considerably cooler than this 200 C. This is desirable, because the differential thermal expansion coefficients between the coating and metal substrates can cause severe mechanical stress.

The yttria was obtained in tablet form from the Cerac Corp. A thin skin at the surface of the evaporant melted during its deposition with an electron beam. At the conclusion of an evaporation, however, the tablets had crumbled to a powder and hence could not be reused. The same technique of bleeding in oxygen was used for the Y_2O_3, as for the HfO_2.

A relatively slow evaporation rate was used for the Y_2O_3. The indicated rate was 0.3 nm (physical thickness) per second. The *indicated* in the previous sentence means that we are not certain about the physical density of the yttria films, since the density must be known to calibrate the quartz crystal microbalance that was used to determine the rate.

2.5 Stabilization by baking

As mentioned in a previous section, the oxide materials were deposited onto substrates that were

relatively hot (250°C) and in a residual oxygen atmosphere. Several investigations [2,3] have shown that the residual oxygen and higher temperature produces films with nigher refractive indices and lower optical absorption.

Both multilayer mirrors and single layers were deposited. The refractive index of the latter were determined as outlined in 3.1. The single layers were baked to reduce the absorption still further via more complete oxidation. The films were initially removed from the evaporation chamber and the reflectance and transmittance were measured via the procedure listed in section 3.2. The black paint was then removed from the uncoated side of the substrate and films were inserted in a furnace and baked at 400°C in air for approximately 14 hours.

After removal from the furnace, they were allowed to stabilize at room temperature for at least two days. This allowed water vapor and other contaminants to come to equilibrium with the matrix of the film. The radiant reflectance and transmittance were then redetermined. The effect of baking is discussed further in 3.4.

2.6 Reflectance and transmission measurements

The radiant reflectance R and transmittance T were measured for several reasons: (a) To determine the refractive index versus wavelength of the coating materials; and, (b) To determine the reflectance and losses in multilayer mirrors.

It is well known that $R \neq 1-T$ for so-called "dielectric" mirrors due to scattering and absorption losses. The reflectance was measured by the V-W attachment on the Cary model 14 spectrophotometer. It should be emphasized that the precision is limited to $\pm 0.5\%$. The experimental uncertainty should be kept in mind when some of the spectral reflectance curves in future sections are observed. Some of the coatings manifest reflectances in excess of 99.5%. It would have been presumptuous to claim that R actually attained a value of 99.8%. There is evidence that it exceeded 99.5%.

3. Optical properties of materials

3.1 Introduction

Little is known about the refractive index versus wavelength of many of the coating materials cited in 2.4. We measured their refractive indices under the evaporation conditions that we had used. The refractive index data, along with the extinction coefficients, will enable the user to compute precisely the reflectance and transmittance versus wavelength of bandpass filters, multilayer polarizers and mirrors composed of these oxides and fluorides.

3.2 Deposition and measurements

We assumed that the dielectric films could be characterized as optically homogeneous materials that had a refractive index $\underline{n}$ and an extinction coefficient $\underline{k}$

written in terms of the complex optical constant $\underline{n}$-$i\underline{k}$. The following procedure was used to determine $\underline{n}$ and $\underline{k}$ as a function of wavelength.

(a) The film was deposited upon a fused silica substrate, as described in section 2.

(b) After its removal from the vacuum it was allowed to sit in ambient atmosphere for approximately eight hours to absorb water vapor and thus attain equilibrium in its optical properties.

(c) The reflectance and transmittance were then measured on a Cary 14 spectrophotometer.

The next section describes how the R and T were translated into $\underline{n}$ and $\underline{k}$ values.

3.3 Data reduction

The first step was to correct for the transmission loss at the nonobverse side of the substrate. The transmittance of the film $\underline{T_f}$ is

$$T_f \cong T_m \frac{(1 - R)}{1 + R(1 - T_m)} \qquad (1)$$

where $\underline{R}$ is the radiant reflectance at the air-substrate interface and $\underline{T_m}$ is the measured transmittance. This equation is derived in section 5. The uncoated side of

the substrate was blackened after the transmission measurements had been made. This blackening suppressed the unwanted Fresnel reflection from the nonobverse side of the substrate. The density on the chart recorder was fed directly into a computer program that found the best fit by a regression technique. The following equation was used for R

$$R = \frac{a_o \cos^2\beta + a_2 \sin^2\beta}{a_1 \cos^2\beta + a_3 \sin^2\beta} \qquad (2)$$

where

$$a_o = (n_o - n_s)^2 \qquad (3)$$

$$a_1 = (n_o + n_s)^2 \qquad (4)$$

$$a_2 = (n - n_o n_s/n)^2 \qquad (5)$$

$$a_3 = (n + n_o n_s/n)^2 \qquad (6)$$

$$\beta = 2\pi\sigma\, nh \qquad (7)$$

where $\underline{n}_o$, $\underline{n}_s$, and $\underline{n}$ are the refractive indices of the incident medium, substrate, and film, respectively. $\underline{h}$ is the metric thickness of the film and σ is the vacuum wavenumber of the incident flux.

A Sellmaier type dispersion equation was assumed for the film index:

$$n^2 = A + B\,\sigma^2 \quad . \qquad (8)$$

The regression algorithm adjusted the constants A and B in the foregoing equation, as well as the metric thickness, until the defect function was minimized.

3.4 Refractive index

Figures 2 to 9 plot the radiant reflectance and the transmittance of four of the oxides that were coated in this study. These include hafnium dioxide, yttrium sesquioxide, tantalum pentoxide and lanthanum sesquioxide.

The spectral reflectance and transmittance, both before and after the baking process, are depicted on the same graph for comparison. One of the main features is that the baking reduces the maximum reflectance. This is evidence that the refractive index was decreased by the baking. Another feature is a decrease in the transmittance at the ultraviolet wavelength where the film has a substantial absorption.

Figures 10, 11, 12 and 13 depict the computed refractive index for the four metal oxides that were studied.

Table 3-1 shows the computed fit to the coefficients in the Sellmaier dispersion polynomial. As mentioned earlier, in almost all cases, the baking decreased the refractive index. This is manifested in Table 3-1 by

Figures 2 through 9

The measured reflectance R and transmittance T for films of hafnium dioxide, yttrium sesquioxide, tantalum pentoxide, and lanthanum sesquioxide, respectively. The solid curve is the prebake measurement. The broken curve is the film after baking for 14 hours at 400°C in air.

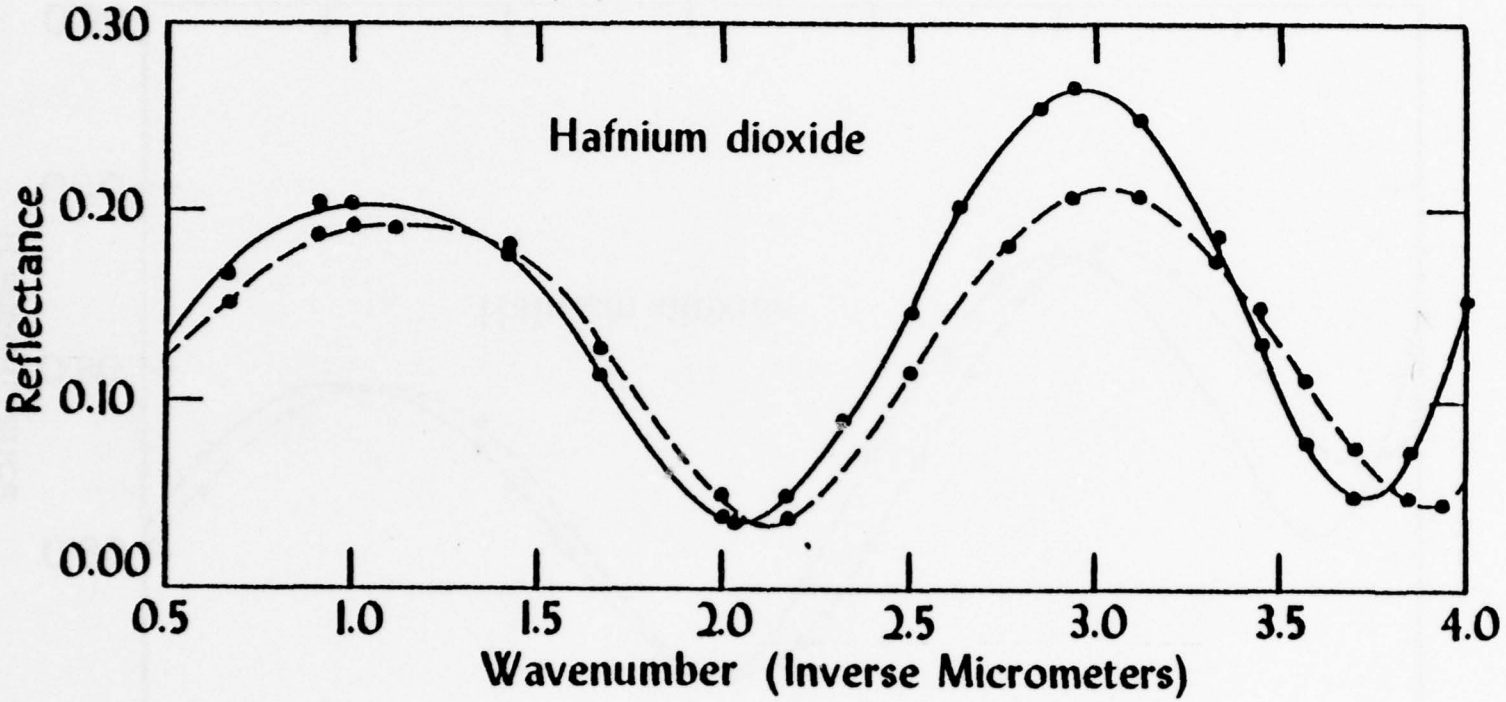
Hafnium dioxide
Reflectance
0.30
0.20
0.10
0.00
0.5
1.0
1.5
2.0
2.5
3.0
3.5
4.0
Wavenumber (Inverse Micrometers)

Fig. 2

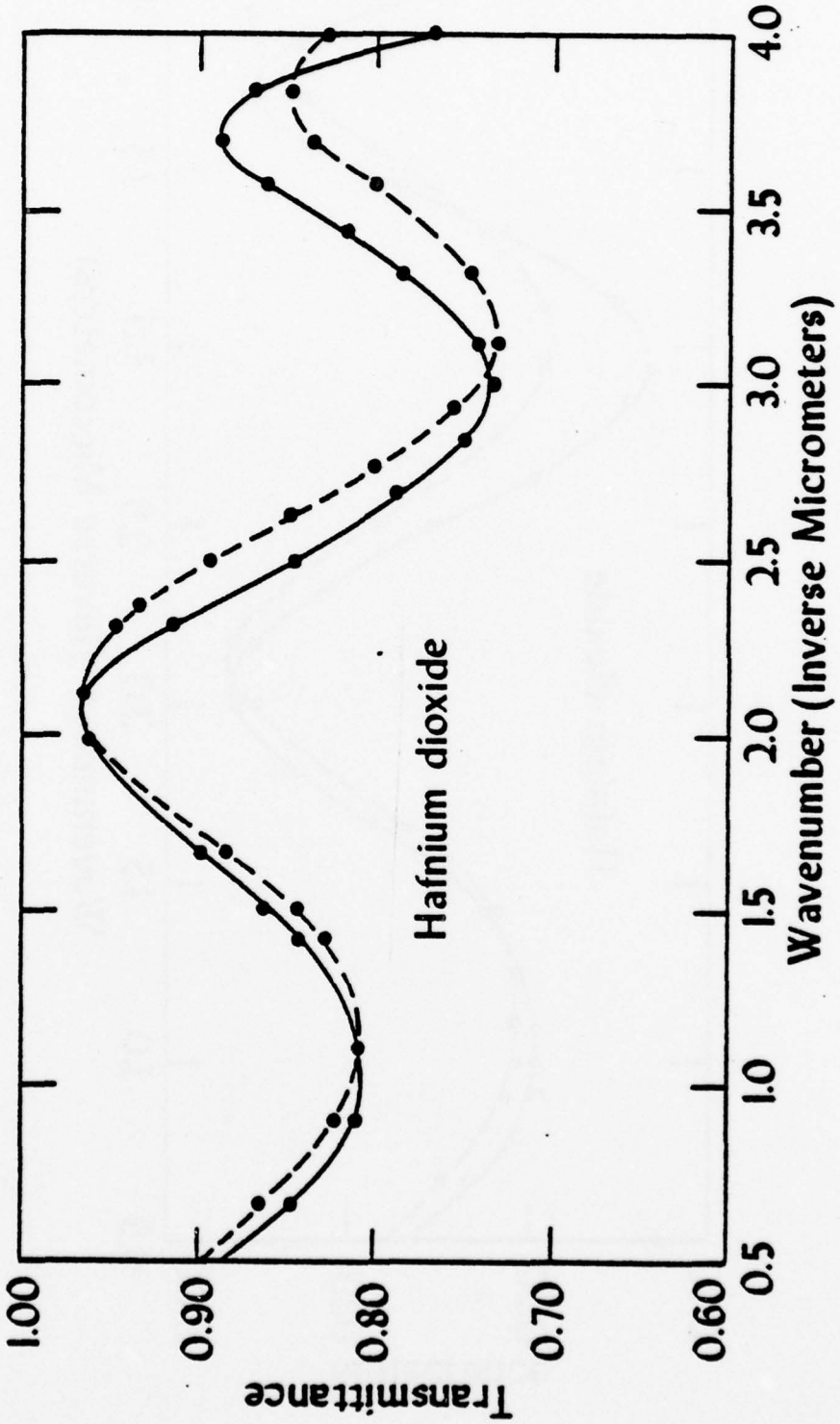
Hafnium dioxide
Transmittance
1.00
0.90
0.80
0.70
0.60
0.5
1.0
1.5
2.0
2.5
3.0
3.5
4.0
Wavenumber (Inverse Micrometers)

Fig. 3

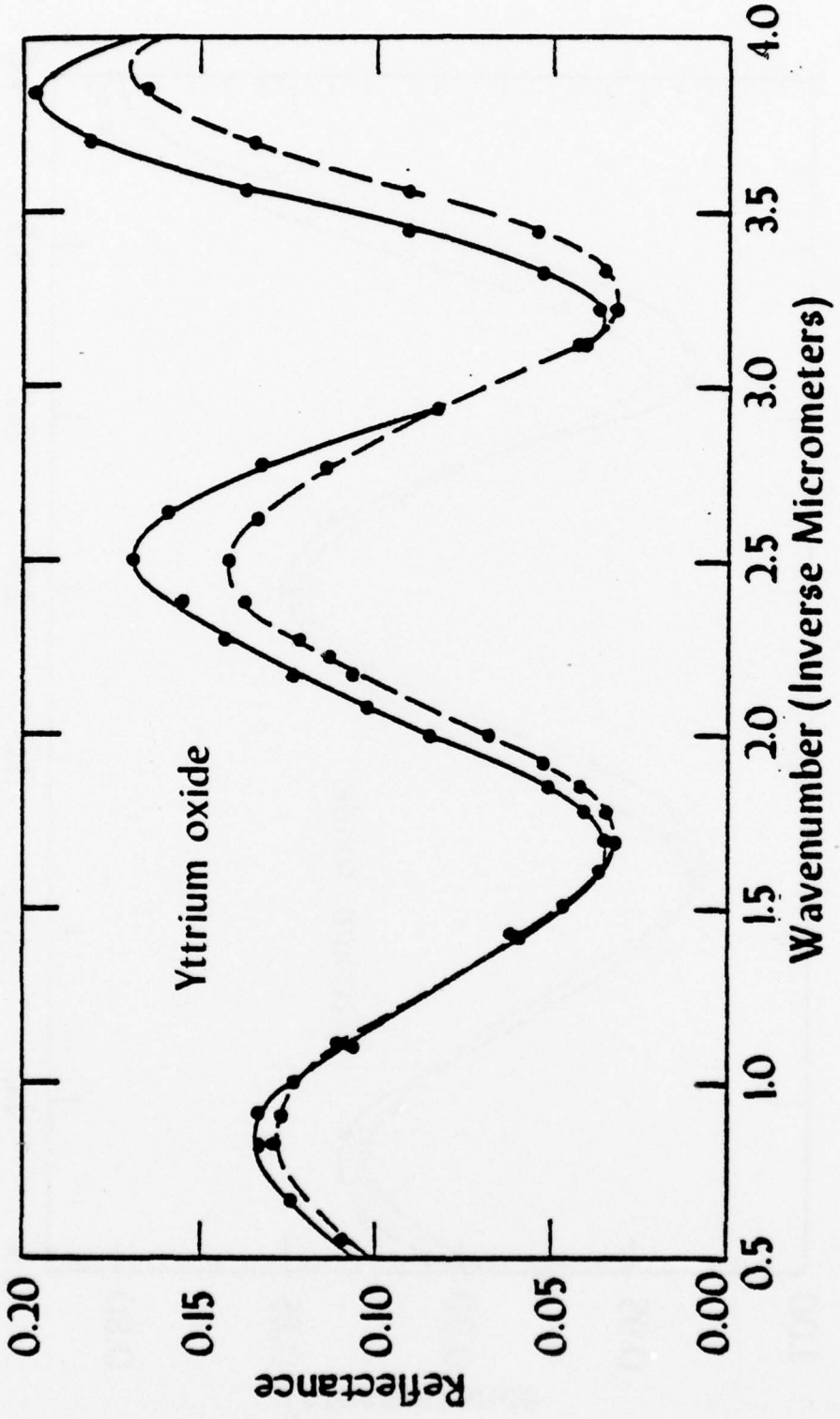
Yttrium oxide
Reflectance
0.20
0.15
0.10
0.05
0.00
0.5
1.0
1.5
2.0
2.5
3.0
3.5
4.0
Wavenumber (Inverse Micrometers)

Fig. 4

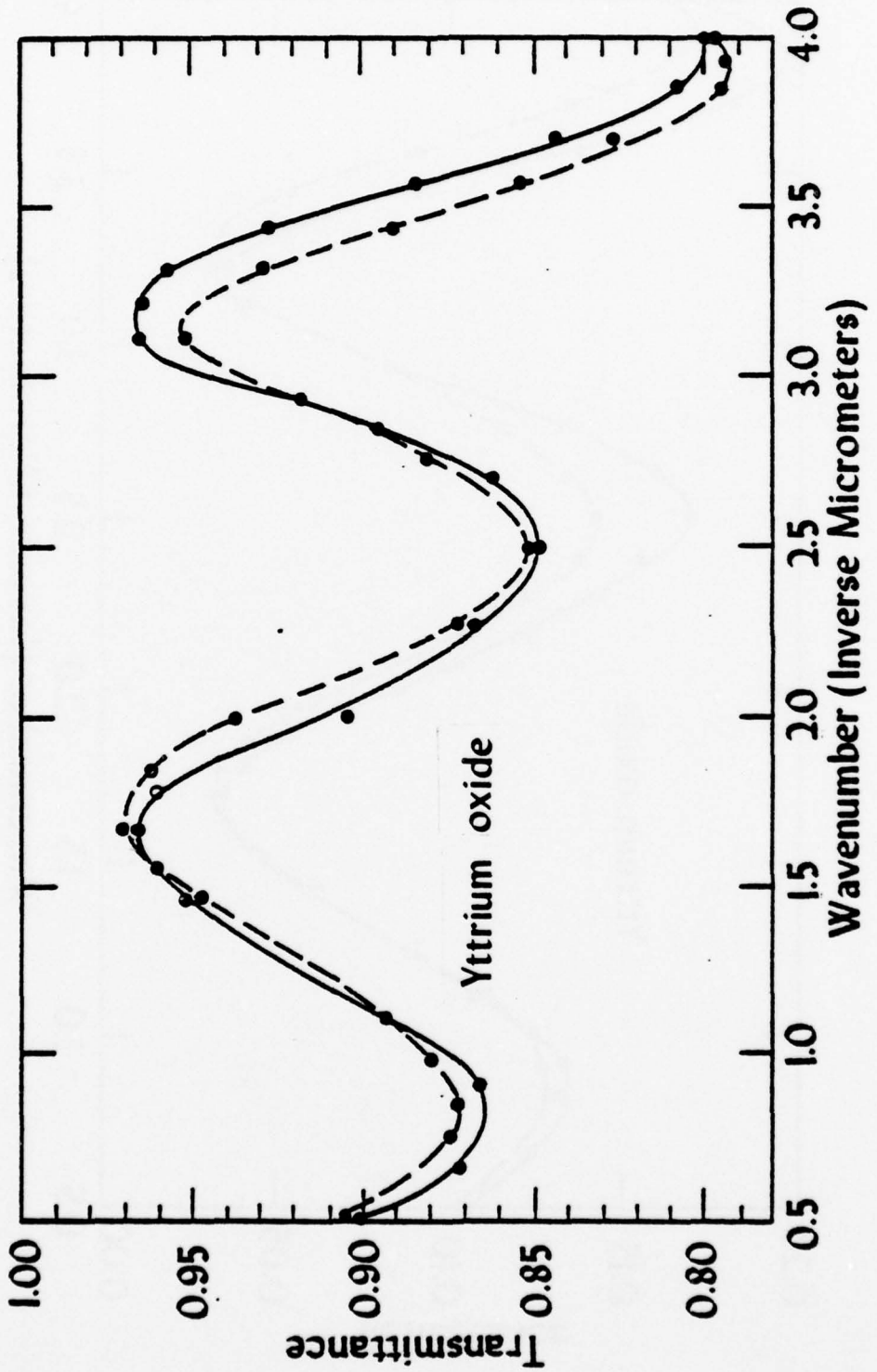
Transmittance
1.00
0.95
0.90
0.85
0.80
0.5
1.0
1.5
2.0
2.5
3.0
3.5
4.0
Wavenumber (Inverse Micrometers)
Yttrium oxide

Fig. 5

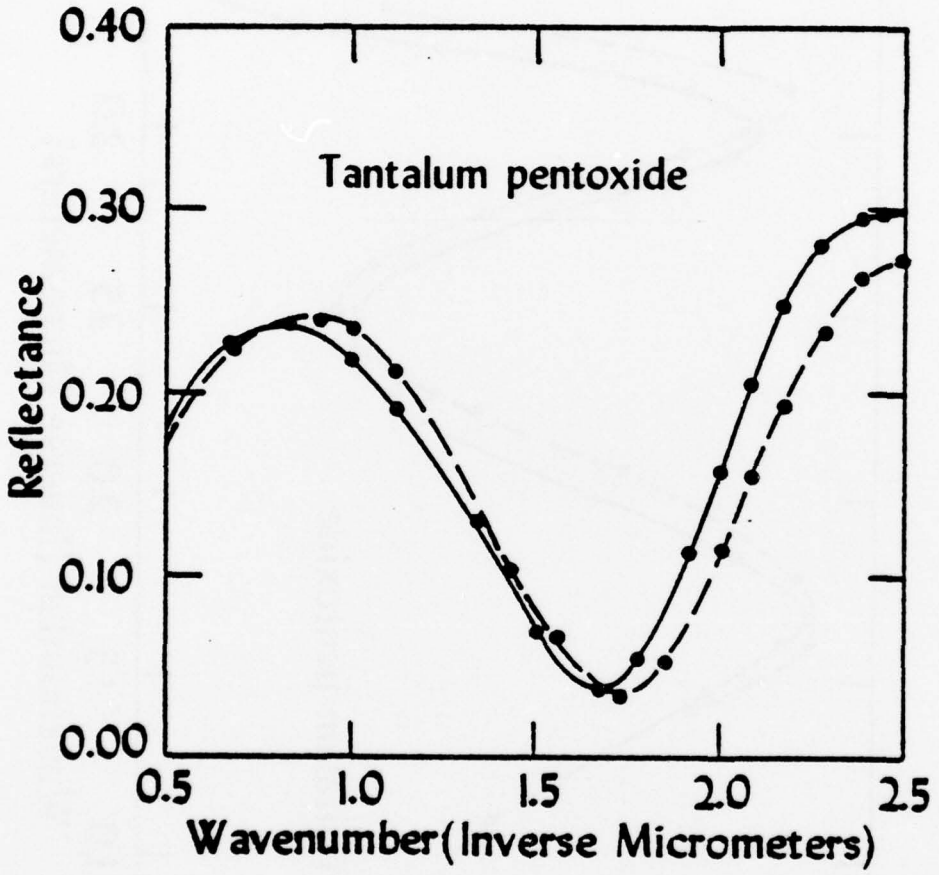
Tantalum pentoxide
Reflectance
0.40
0.30
0.20
0.10
0.00
0.5
1.0
1.5
2.0
2.5
Wavenumber(Inverse Micrometers)

Fig.6

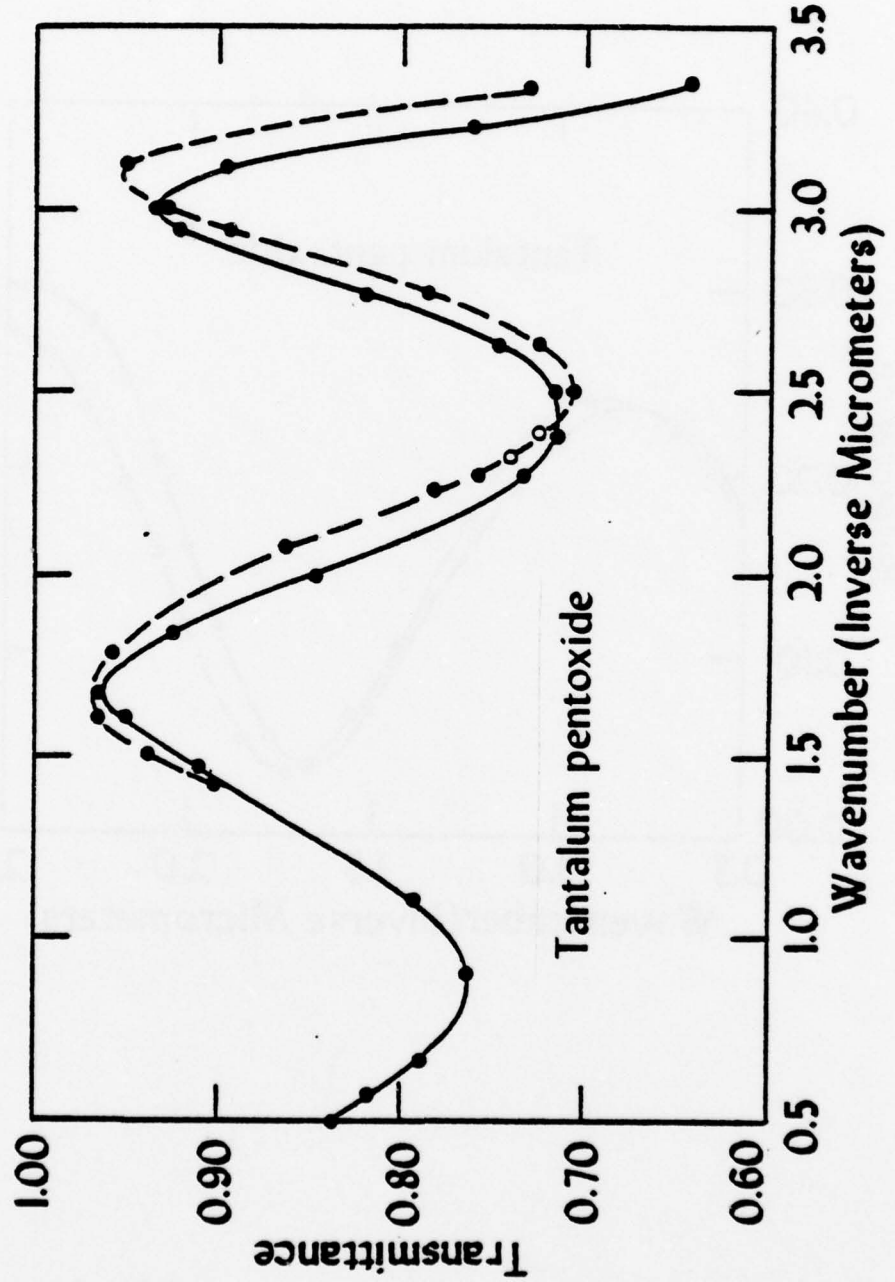
Transmittance
1.00
0.90
0.80
0.70
0.60
0.5
1.0
1.5
2.0
2.5
3.0
3.5
Wavenumber (Inverse Micrometers)
Tantalum pentoxide

Fig.7

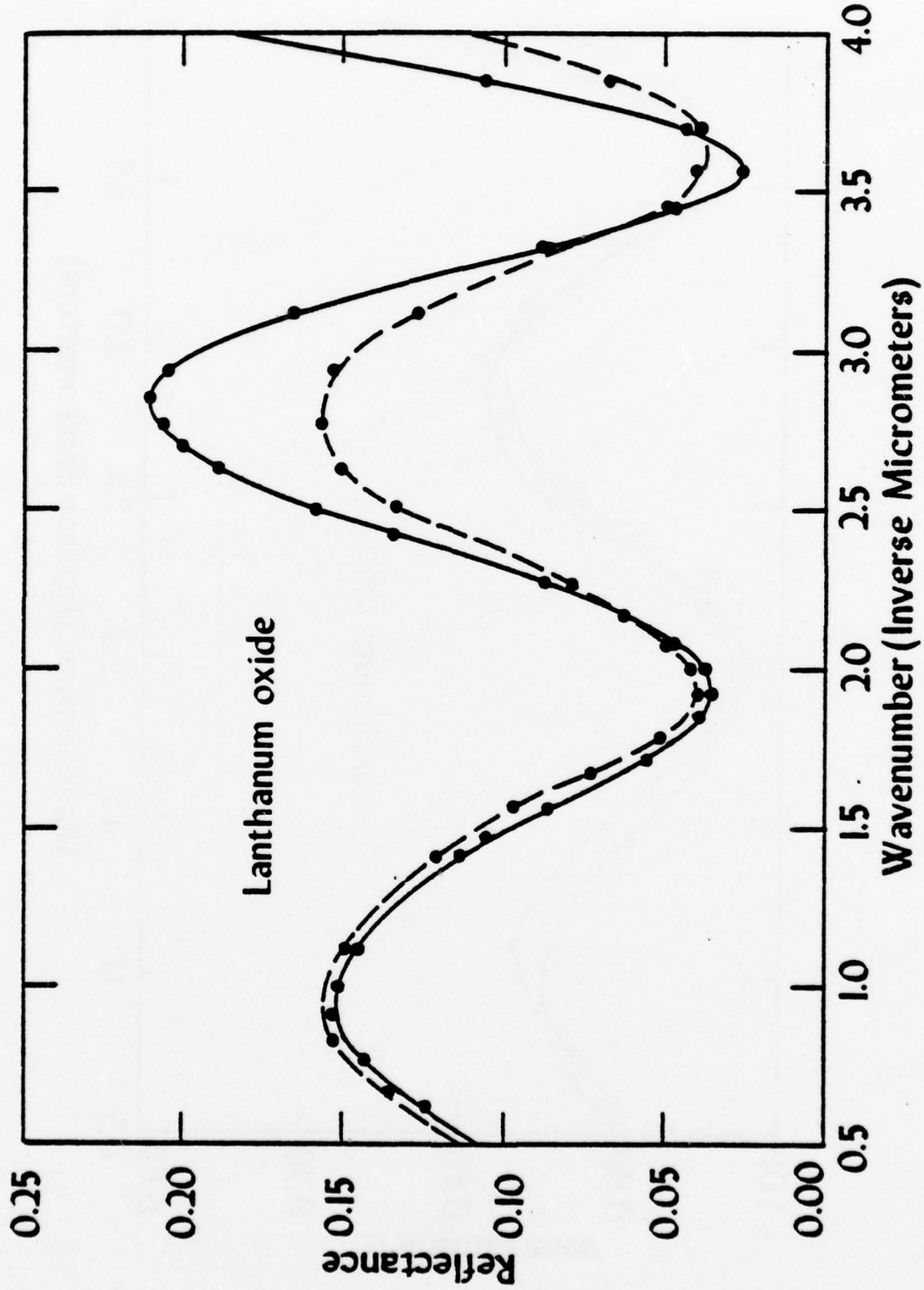
Lanthanum oxide
Reflectance
0.25
0.20
0.15
0.10
0.05
0.00
0.5
1.0
1.5
2.0
2.5
3.0
3.5
4.0
Wavenumber (Inverse Micrometers)

Fig. 8

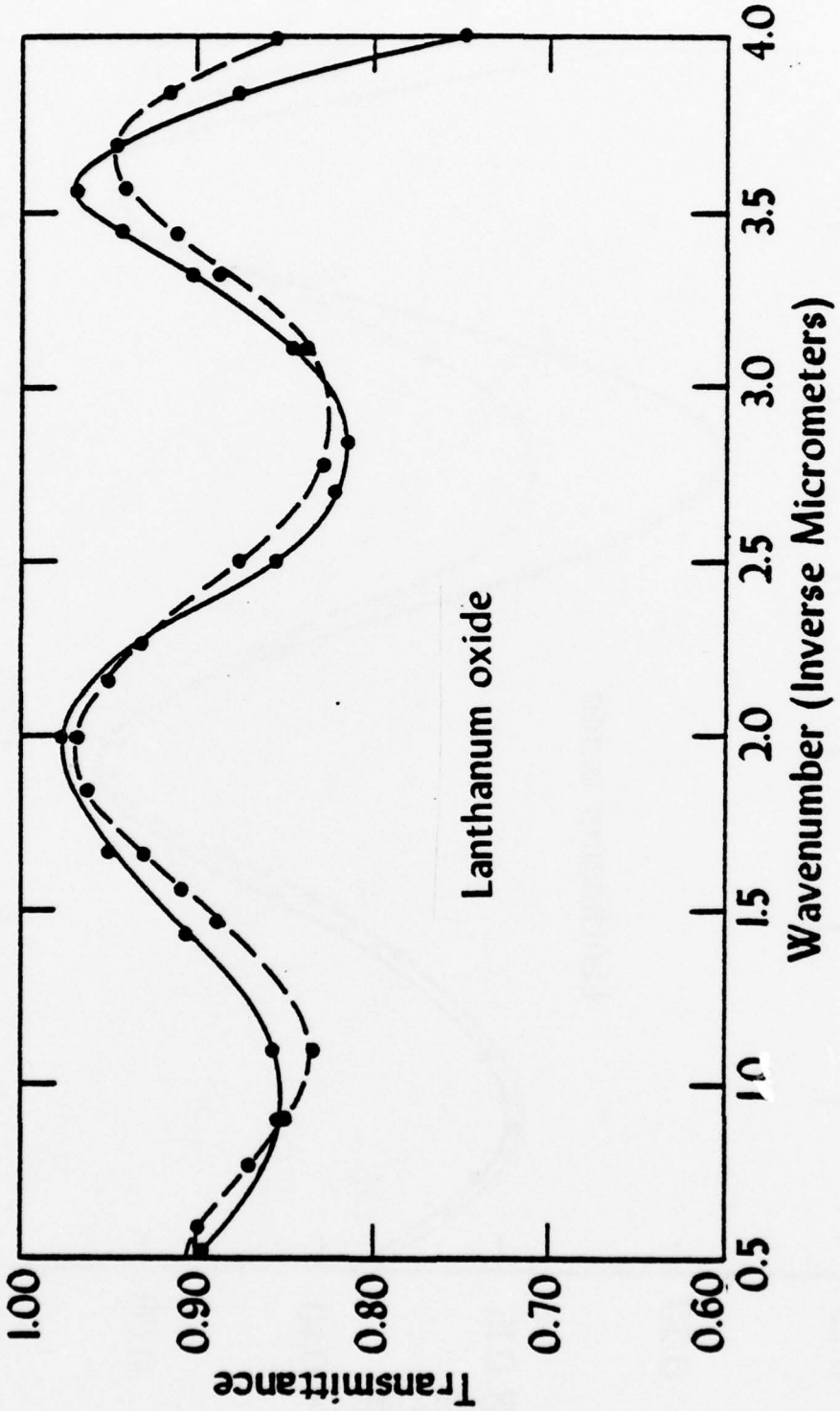
Transmittance
1.00
0.90
0.80
0.70
0.60
0.5
1.0
1.5
2.0
2.5
3.0
3.5
4.0
Wavenumber (Inverse Micrometers)
Lanthanum oxide

Fig. 9

Table 3-1

The optical parameters as determined by the computer

Material	Prebake			Postbake		
	A	B	h in μm	A	B	h in μm
HfO_2	3.8524	0.09188	0.118	3.7467	0.04687	0.120
Y_2O_3	3.1286	0.04195	0.165	3.0322	0.03089	0.170
Ta_2O_5	4.2446	0.13158	0.140	4.2454	0.06677	0.140
La_2O_3	3.3087	0.06952	0.137	3.3723	0.0197	0.142

The least squares determination of the metric thickness h and the dispersion of the refractive index (where the constants A and B appear in Eq. (8) via spectroreflectometry. Postbake refers to baking at 14 h at 400°C in air.

Figures 10 through 13

The refractive index, as computed from spectroreflectrometric data, for hafnium dioxide, yttrium sesquioxide, tantalum pentoxide, and lanthanum sesquioxide, respectively. Curve a corresponds to the prebake measurements. Curve b is after baking at 400°C in air for 14 hours.

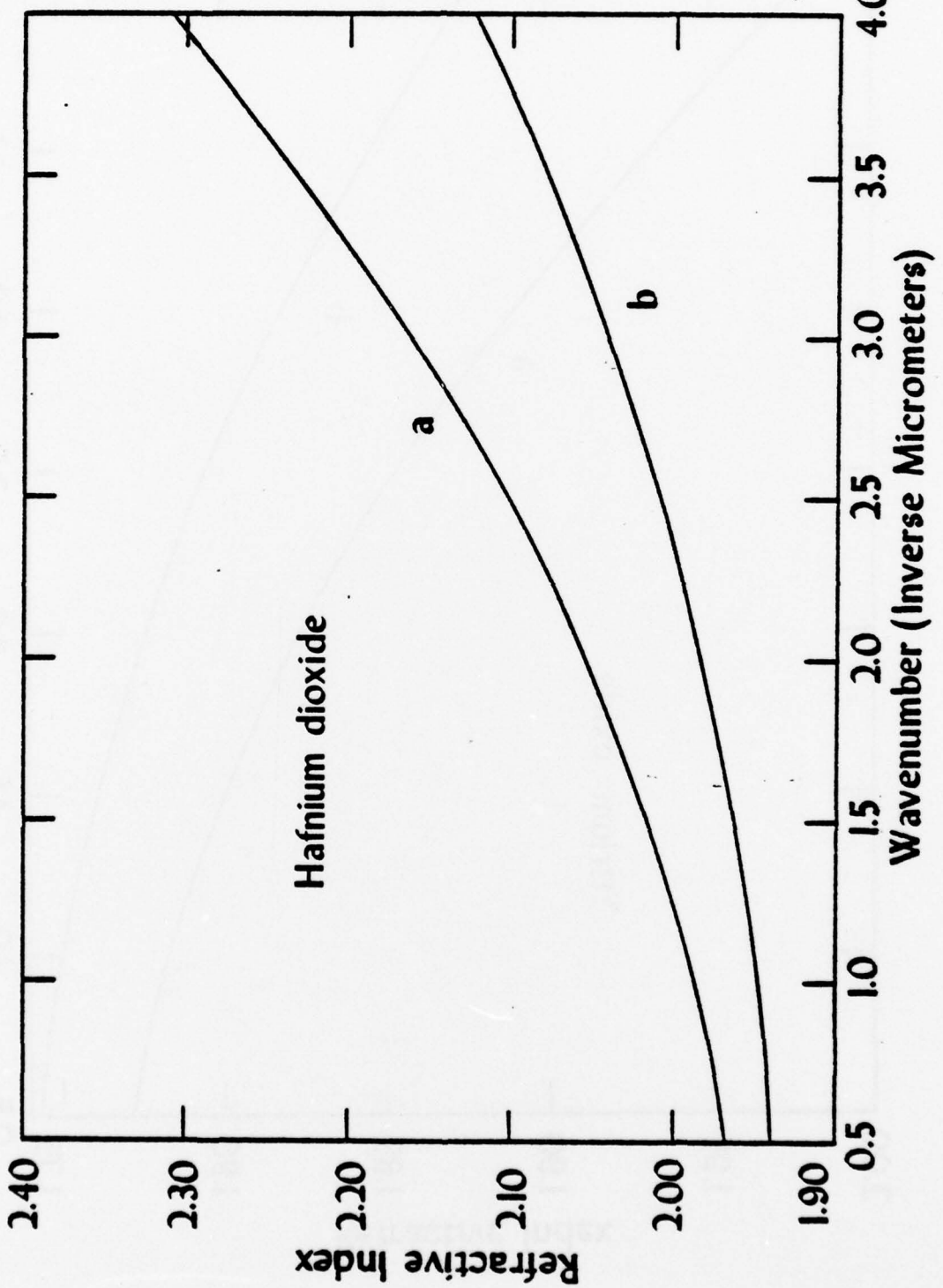
Hafnium dioxide
a
b
Refractive Index
2.40
2.30
2.20
2.10
2.00
1.90
0.5
1.0
1.5
2.0
2.5
3.0
3.5
4.0
Wavenumber (Inverse Micrometers)

Fig. 10

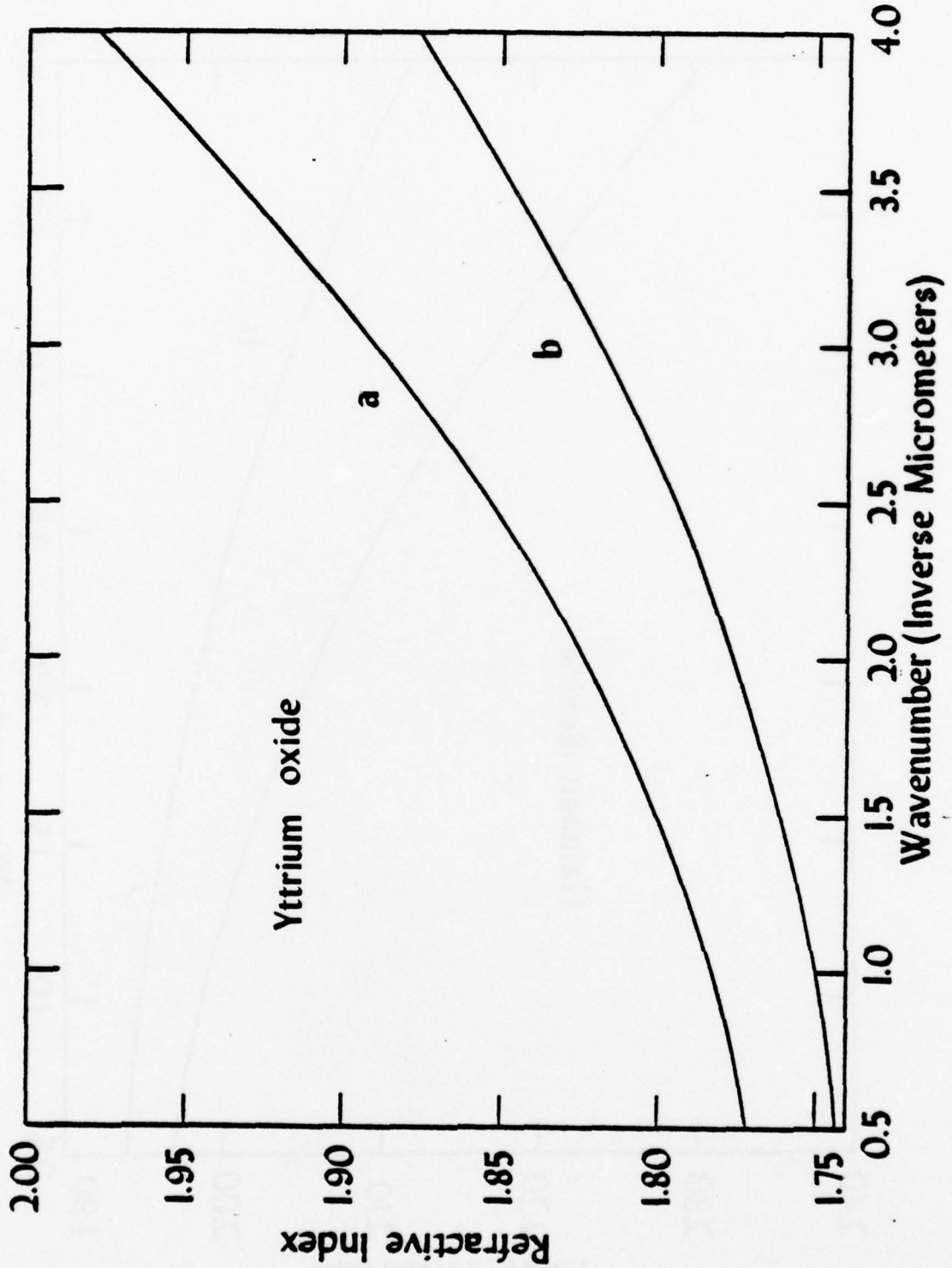
Refractive Index
2.00
1.95
1.90
1.85
1.80
1.75
0.5
1.0
1.5
2.0
2.5
3.0
3.5
4.0
Wavenumber (Inverse Micrometers)
Yttrium oxide
a
b

Fig. 11

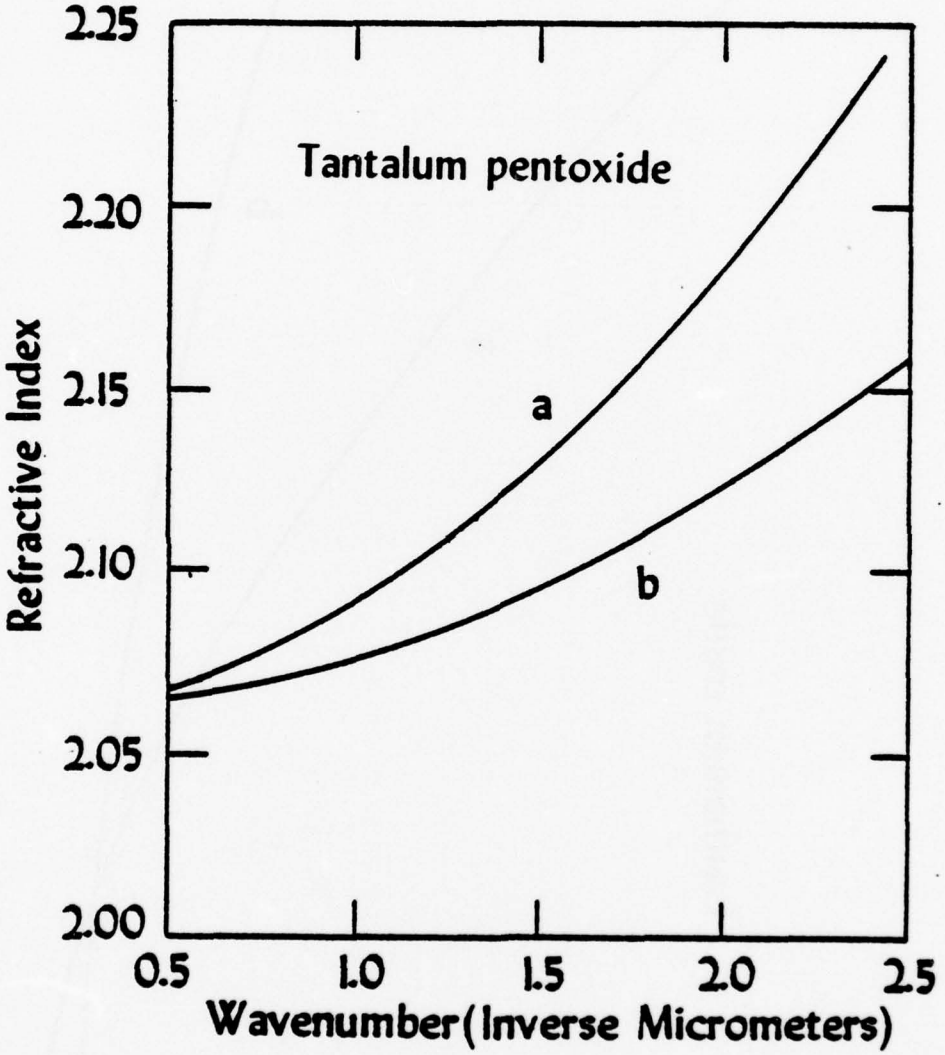
Tantalum pentoxide
a
b
Refractive Index
2.25
2.20
2.15
2.10
2.05
2.00
0.5
1.0
1.5
2.0
2.5
Wavenumber (Inverse Micrometers)

Fig.12

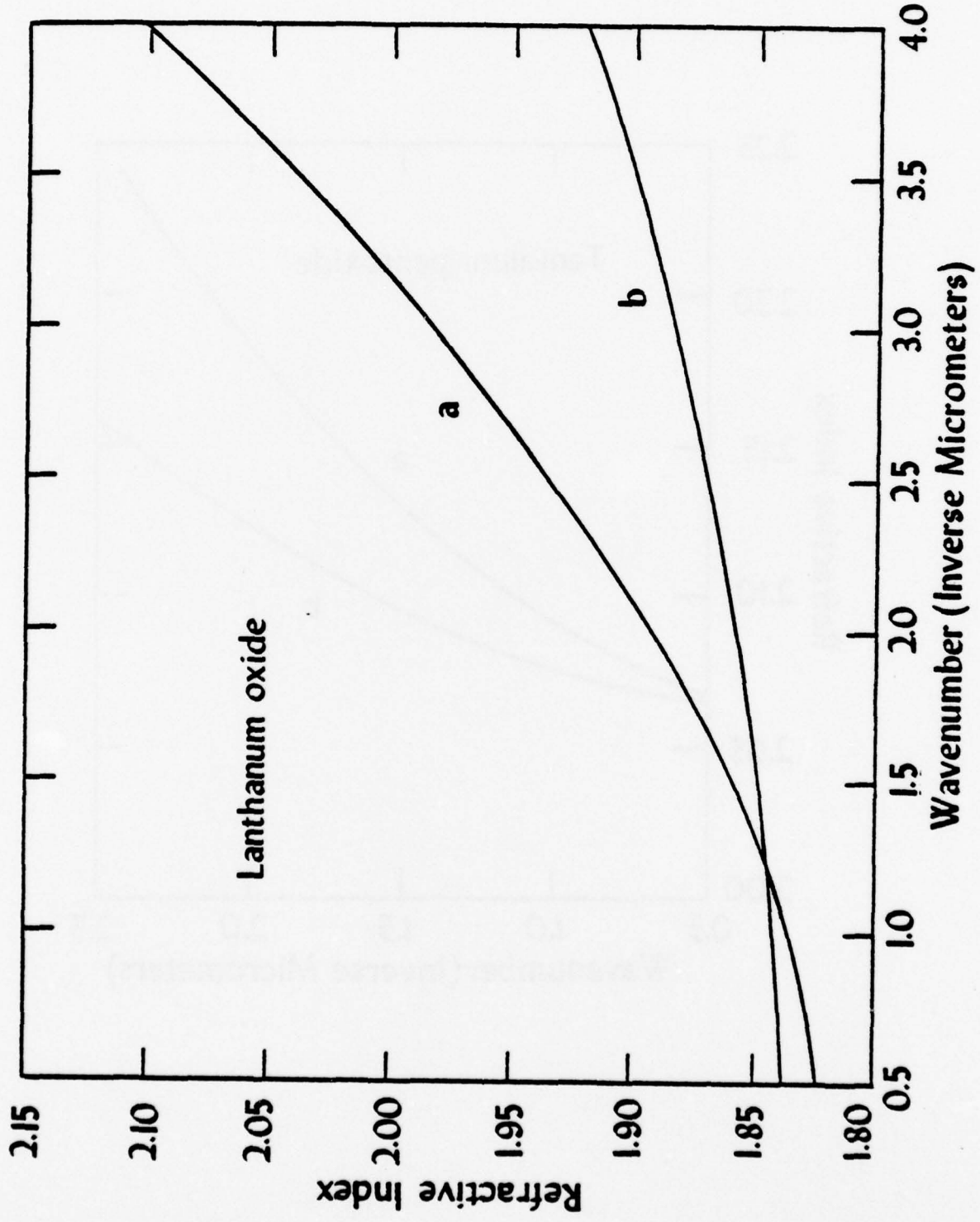
Refractive Index
2.15
2.10
2.05
2.00
1.95
1.90
1.85
1.80
0.5
1.0
1.5
2.0
2.5
3.0
3.5
4.0
Wavenumber (Inverse Micrometers)
Lanthanum oxide
a
b

Fig. 13

the fact that both the A and the B coefficients are less for the post-baked sample than for the prebaked sample.

Finally, there is the question whether the baking for 14 hours at 400°C in air is the optimum treatment. There is evidence that a shorter bake does not fully oxidize the film. For example, Figures 14, 15 and 16 plot the refractive index of a hafnium dioxide film and two separate yttrium oxide films that were baked for four hours at 400°C in air. Comparing these data with those shown in Figs. 10 and 11, it is evident that the refractive index was changed relatively little by the four hour bake as compared to the unbaked sample.

A more vigorous baking of a sample at 700°C for four hours produced a considerable amount of crazing and cracking in the films. It is conjectured that this might be caused by the differential thermal expansion coefficient between the films and the relatively unexpansive silica substrate.

3.5 Extinction coefficient

The extinction coefficient $\underline{k}$ was determined from absoption measurements, as outlined in section 5.2. Due to the experimental uncertainty of $\pm$1% in both $\underline{R}$ and $\underline{T}$, the absorption, and hence $\underline{k}$, could only be determined near 250 nm, as shown in Table 3-2. The lower absorption in the Y_2O_3, as compared to the HfO_2, is patent.

Table 3-2

Material	Prebake		Postbake	
	n	k	n	k
HfO_2	2.307	0.0156	2.2105	0.0218
Y_2O_3	1.9786	0.0043	1.8778	0.0065
La_2O_3	2.102	0.00111	1.920	0.00258

The extinction coefficient k and refractive index n of films as measured after evaporation and after baking at 400°C for 14 h in air. The wavelength is 250 nm.

Figure 14

The computed refractive index for hafnium dioxide. The broken curve corresponds to the postbake measurement. The sample was baked for four h in air at 400°C.

Figures 15 and 16

The computed refractive index for two samples of yttrium sesquioxide. Curve b is the postbake measurement. The samples were baked at 400°C for four h in air.

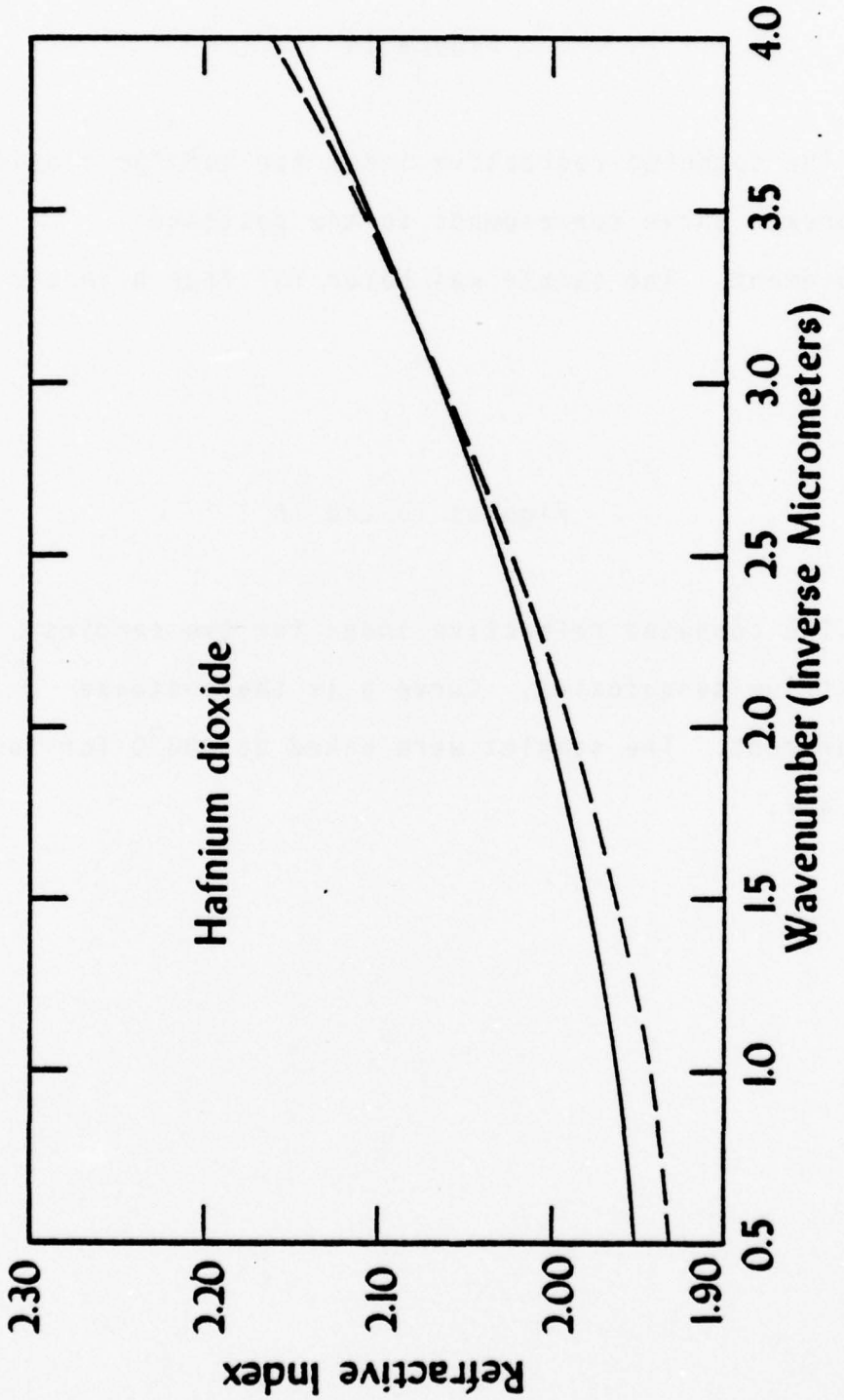
Hafnium dioxide
Refractive Index
2.30
2.20
2.10
2.00
1.90
0.5
1.0
1.5
2.0
2.5
3.0
3.5
4.0
Wavenumber (Inverse Micrometers)

Fig. 14

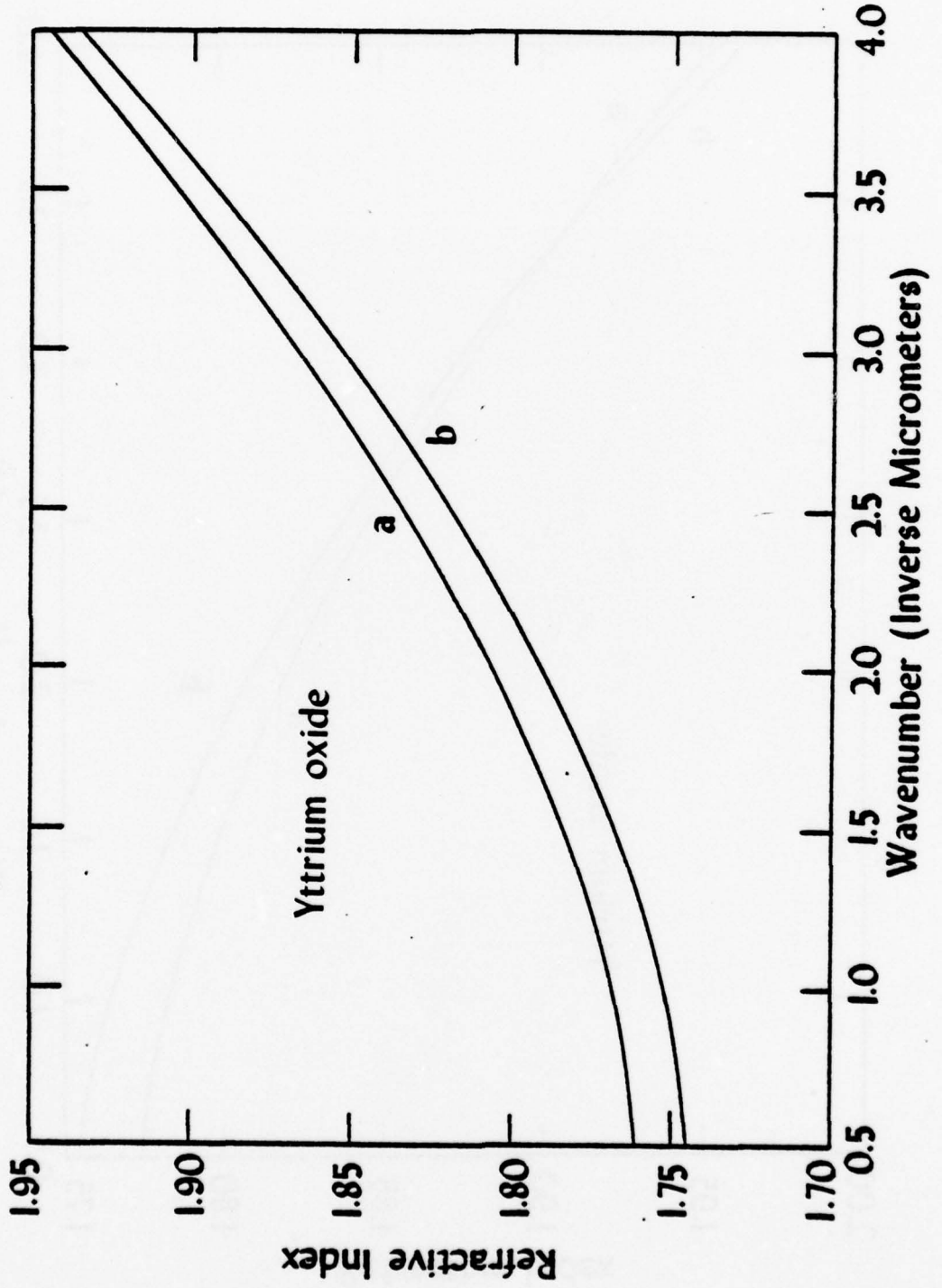
Refractive Index
1.95
1.90
1.85
1.80
1.75
1.70
0.5
1.0
1.5
2.0
2.5
3.0
3.5
4.0
Wavenumber (Inverse Micrometers)
Yttrium oxide
a
b

Fig. 15

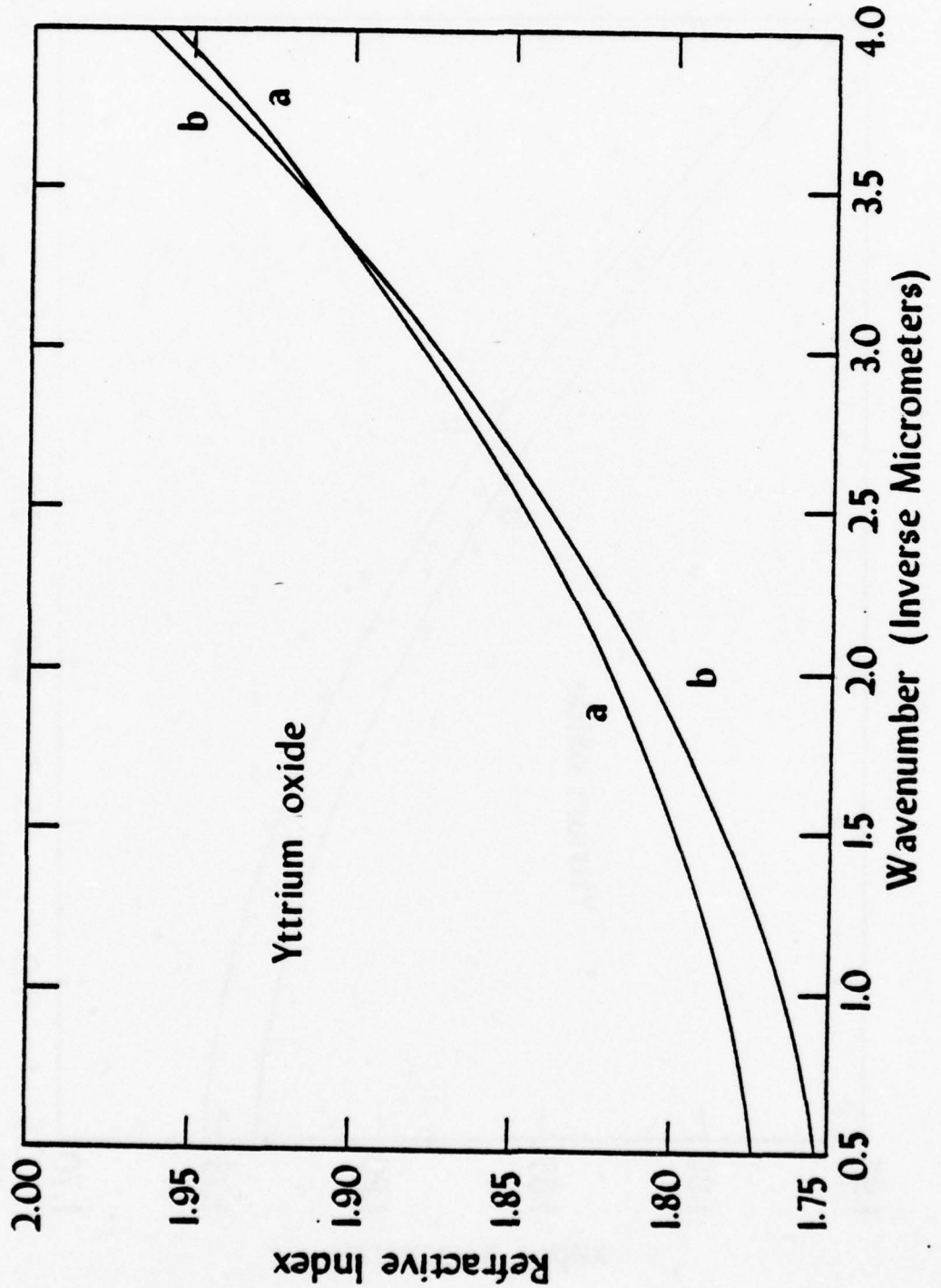
Refractive Index
2.00
1.95
1.90
1.85
1.80
1.75
0.5
1.0
1.5
2.0
2.5
3.0
3.5
4.0
Wavenumber (Inverse Micrometers)
Yttrium oxide
a
b
a
b

Fig. 16

3.6 Discussion of refractive index data

The determination of these refractive indices points to some new ways to construct highly reflecting laser damage resistant multilayer reflectors at 350 nm. Consider, for example, the possible use of tantalum pentoxide as a high index material. From the dispersion polynomial, [Eq. (8)] the A and B coefficients in Table 3-1, we find that the refractive index of baked tantalum pentoxide is 2.19 at 350 nm. This means that seven alternate layers of tantalum pentoxide and silica deposited upon a fused silica substrate would produce a radiant reflectance of 94%. It is doubtful, however, that this reflectance could be attained because of the absorption in the outer layers of the tantalum pentoxide. This is no deterrent, however, because materials that have lower loss, such as yttrium oxide and hafnium dioxide are now used in the high index films at the top of the stack.

What are the advantages of using the tantalum pentoxide for this total reflector? The chief advantage is that the tantalum has little scatter and virtually no mechanical stress. Furthermore, electron diffractographs have shown that films of tantalum pentoxide are amorphous and therefore the stack does not become rougher as more layers are deposited. This technique of using a slightly more absorbing but higher refractive index material at the bottom of the total reflector means that the number

of layers and scattering of the stack will be lower, as compared to a stack in which hafnium dioxide is used exclusively as the high index layer.

4. Properties of reflectors

4.1 Introduction

Multilayer dielectric reflectors at 250 nm and 350 nm were prepared on a host of substrates -- fused silica, polished molybdenum, sputtered molybdenum, and polished silicon carbide. Since these R and T data are well summarized in another report [4], no effort is made to reproduce the R and T curves of even a moiety of the coatings that were produced under this contract.

4.2 Reflectors at λ = 350 nm

As an example of a reflector, Fig. 17 shows the measured spectral reflectance of a multilayer of the design

$$\text{air } (H\ L)^{11}\ H \text{ substrate}$$

where H and L represent, respectively, layers of hafnium dioxide and silica of quarterwave optical thickness at 355 nm. The solid curve is the smoothed data measured at the University of Rochester on a Cary model 14 spectroreflectometer. The solid points are the measurements at Naval Weapons

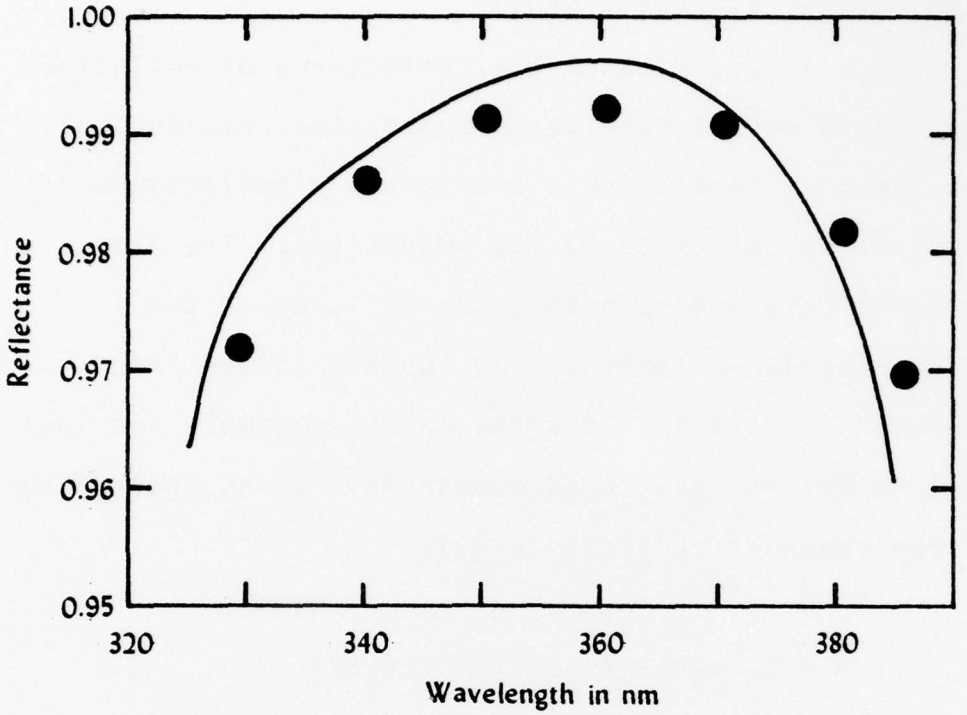

Fig. 17

The measured spectral reflectance of a multilayer of the design

$$\text{air } (H\ L)^{11}\ H \text{ substrate}$$

where H and L represent, respectively, layers of hafnium dioxide and silica of quarterwave optical thickness at 355 nm. The solid curve is the smoothed data measured at the University of Rochester on a Cary model 14 spectroreflectometer. The solid points are the measurements at Naval Weapons Center, China Lake, California.

Center, China Lake, California.

Figs. 18 and 19 show the reflectance of reflectors on sputtered Mo and massive Mo substrates, respectively. It is tempting to attribute the superior reflectance of the sputtered substrate to its smoothness. The data from China Lake indicate that the variance of the surface profile -- commonly and loosely called "rms roughness" -- is 4.7 nm for the polished sample and less than 1 nm for the sputtered substrate. Using these data, [5] the specular reflectance $\underline{R}$ is

$$R = R_0 \exp(-(4\pi \sigma /\lambda)^2 = 0.973 \qquad (9)$$

for λ= 355 nm, σ= 4.7 nm and R_0 = 1.0. Our measured reflectances exceeded this, but it can be argued that the measured biconical reflectance collected low-angle scattering and hence does not resemble the "specular" reflectance cited above.

4.3 Reflectors at 250 nm.

Figure 20 shows the reflectance of a 24 layer coating of the design:

$$\text{air } (H\ L)^{12} \text{ substrate}$$

where substrate is SiC. The H and L layers are HfO_2

Captions to Figs. 18 and 19

The measured reflectance of multilayers of the design

$$\text{air } (H\ L)^{11} \text{ substrate}$$

where H and L represent layers of quarterwave optical thickness (at λ = 355 nm) of hafnium dioxide and silica, respectively. The substrate is sputtered molybdenum (Fig. 18) and polished Mo (Fig. 19).

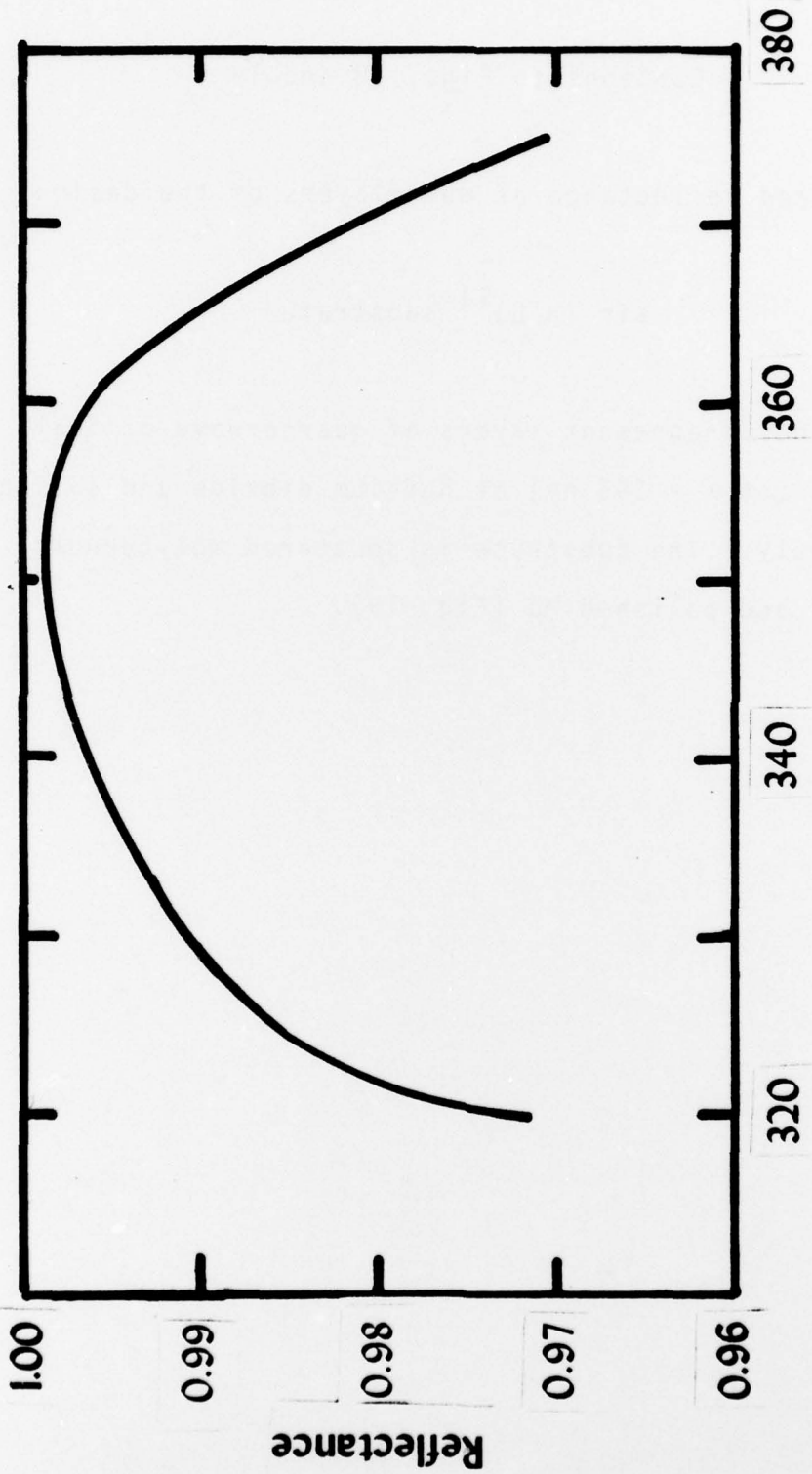
1.00
0.99
0.98
0.97
0.96
Reflectance
320
340
360
380
Wavelength in nm

Fig. 18

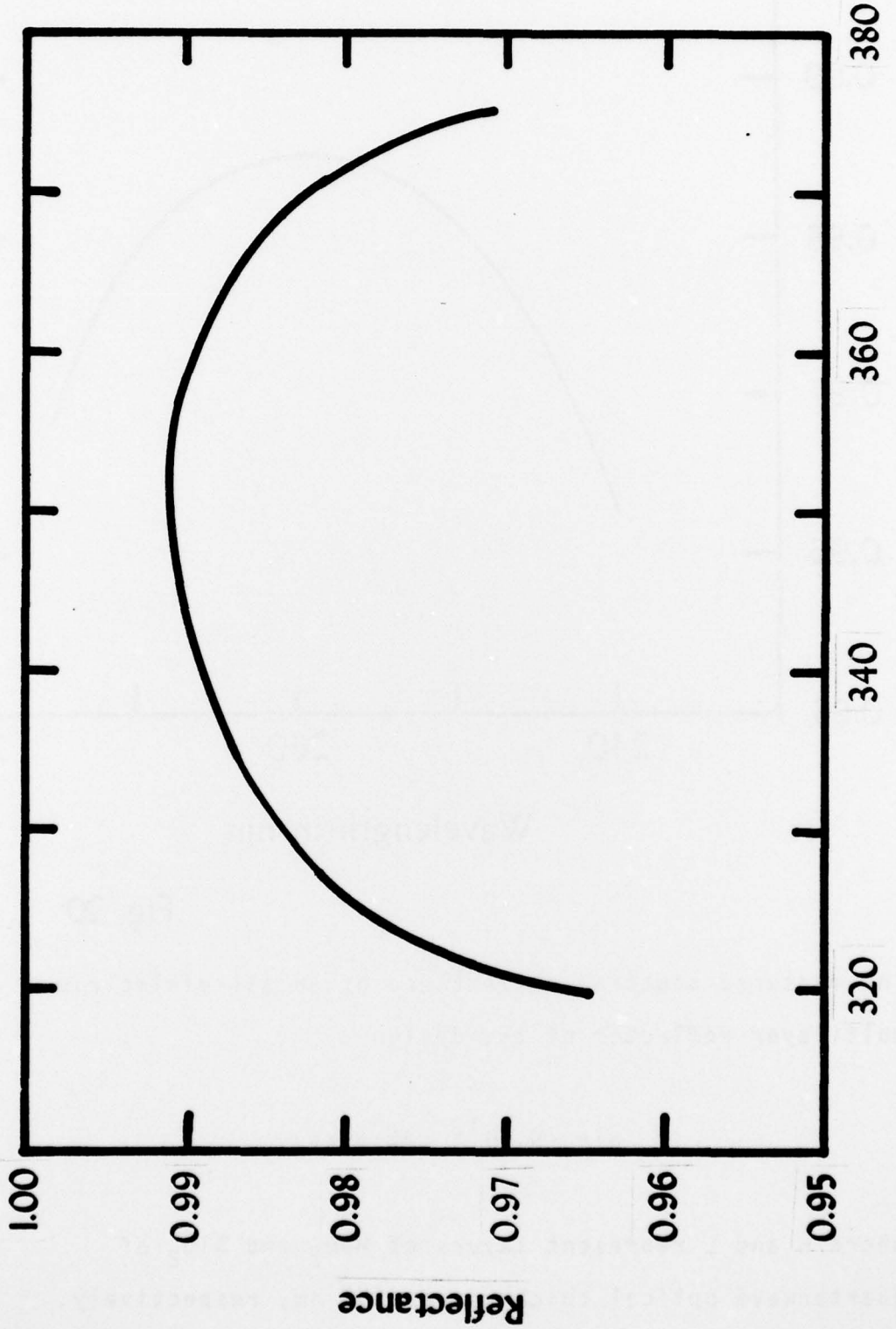
1.00
0.99
0.98
0.97
0.96
0.95
Reflectance
320
340
360
380
Wavelength in nm

Fig. 19

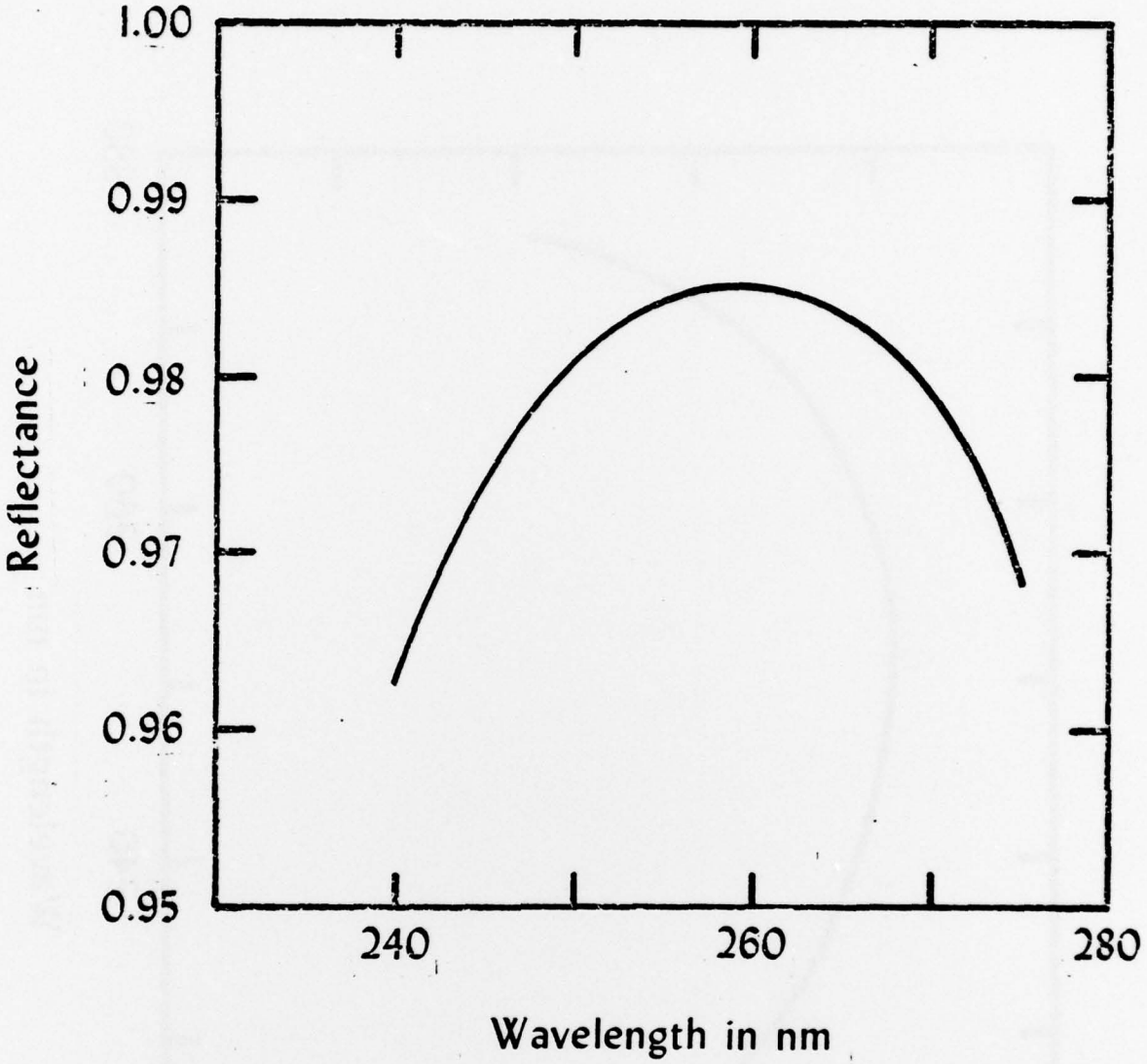

Fig. 20

The measured spectral reflectance of an all-dielectric multilayer reflector of the design

$$\text{air } (H\ L)^{12} \text{ substrate}$$

where H and L represent layers of HfO_2 and SiO_2 of quarterwave optical thickness at 255 nm, respectively. The substrate is silicon carbide.

and SiO_2, respectively. We assumed that the HfO_2 was absorbing and hence the limiting factor in attaining 0.999 reflectance.

The first approach was to deposit a stack of hafnia and silica, and then to overcoat it with a stack of yttria and silica. The design was

$$\text{air } Y\ (L\ Y)^6\ (L\ H)^9 \text{ substrate}$$

where L is a low index layer of silica whose optical thickness is approximately a quarterwave at 250 nm. Y and H represent yttria and hafnia layers respectively, with the same optical thickness as the silica. As shown in Fig. 21, its reflectance is in excess of 99% at 250 nm. The foregoing stack contains 31 layers.

There is strong evidence that the losses in the layers at the top of the stack limit the reflectance. For example, Figure 22 shows the spectral reflectance of the design

$$\text{air } (Y\ L)^{17}\ Y \text{ substrate}$$

where Y and L have the same meaning as in the previous paragraph. This stack is composed entirely of yttria and silica. As shown in Fig. 22, its peak reflectance is approximately the same as that of the stack with the hafnia on the bottom. In the absence of absorption, one

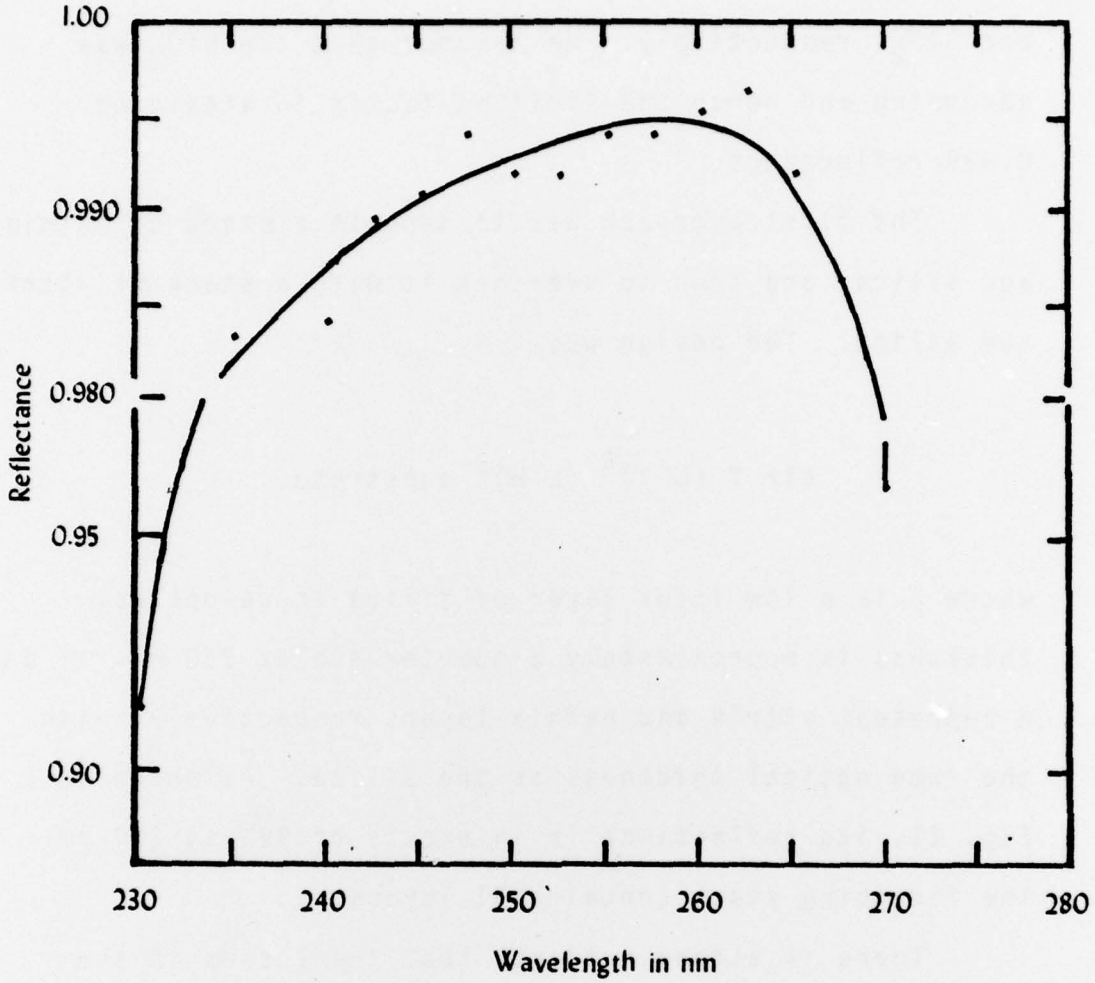

Fig. 21

The measured spectral reflectance (on a Cary model 14 spectroreflectometer) of a multilayer of the design

$$\text{air } Y\ (L\ Y)^6\ (L\ H)^9 \text{ substrate}$$

where H, Y, and L represent layers of hafnia, yttria, and silica, respectively, of quarterwave optical thickness at 250 nm. The ordinate changes scale at 0.98.

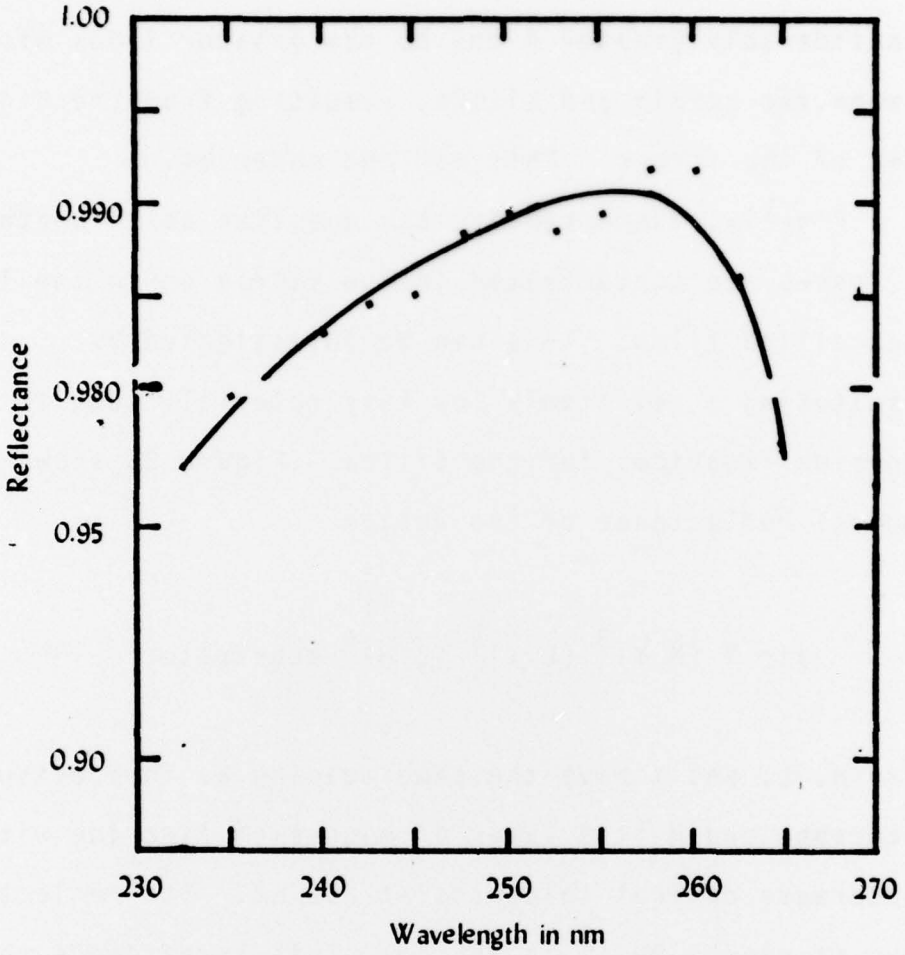

Fig. 22

The caption to Fig. 21 obtains, with the exception that the design of the multilyaer is

$$\text{air } Y\ (L\ Y)^{17} \text{ substrate}$$

would expect that the stack with the hafnia should have a considerably greater R due to the greater index mismatch between the hafnia and silica, resulting from the higher index of the former. This was not observed.

Finally, there remains the question as to whether the losses are concentrated in the yttria or in the low index silica films. This can be investigated by substituting a relatively low loss material, such as magnesium fluoride, for the silica. Figure 23 shows the spectral reflectance of the design

$$\text{air } Y\ (M\ Y)^3\ (L\ Y)^5\ (L\ H)^9 \text{ substrate}$$

where H, L, and Y have the same meaning as in previous paragraphs and M is a layer of magnesium fluoride with a quarterwave optical thickness at 250 nm. Its reflectance peaks at nearly 99.4% at 255 nm. This is evidence that the yttria is a major contributor to the absorption at 250 nm. The reason is that the index of the magnesium fluoride is considerably lower than the silica at this wavelength. For example, the MgF_2 index is 1.40 and the silica is 1.55. There is a considerably greater index mismatch between the magnesium fluoride and the yttria layers, which in turn produces a higher reflectance -- provided there are no absorption and/or scattering losses, of course. The fact that the reflectance of this type of stack is not appreciably different than one in which SiO_2

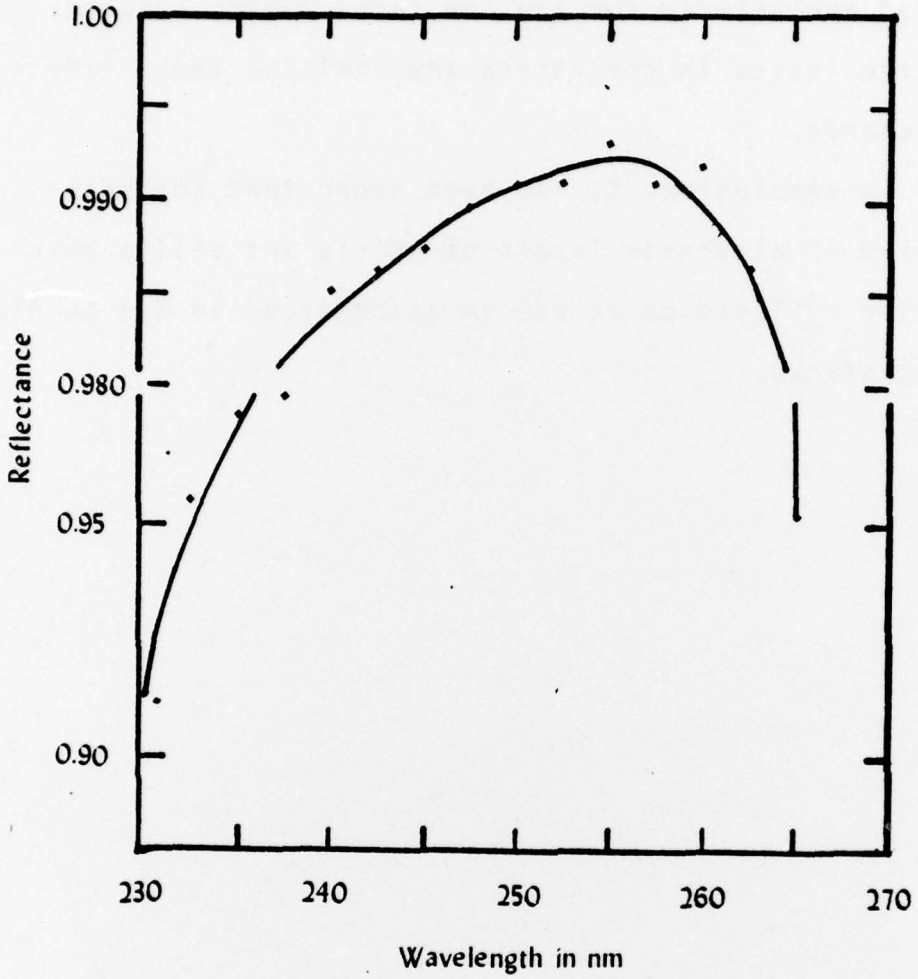

Fig. 23

The caption to Fig. 21 obtains, with the exception that the design of the multilayer is

$$\text{air } Y\ (M\ Y)^3\ (L\ Y)^5\ (L\ H)^9 \text{ substrate}$$

H, L, and Y have the same meaning as in the caption to Fig. 21, and M represents a layer of magnesium fluoride whose optical thickness is a quarterwave at 250 nm.

is used exclusively for the low index layer, suggests that the losses in the yttria are limiting the ultimate reflectance.

In conclusion, it has been shown that the stacks composed of alternate layers of yttria and silica have superior reflectance at 250 nm as compared in the hafnia/silica stacks.

5. Appendices

5.1 Determination of the transmittance of the film via a double-beam ratio-recording spectrophotometer.

Equation (1) cited in section 3.3 is an approximation. Although it has appeared in the literature [6,7], it is useful to rederive it in order to see if the approximations are valid under the conditions of our usage.

An uncoated identical substrate is placed in the reference beam. The notation is shown in Fig. 24. We define:

T_s = Transmittance through the substrate/air interface

T_f = Transmittance of the evaporated layer

T_{ss} = Transmittance of the bare substrate

T_{fs} = Transmittance of film and substrate

T_m = Transmittance, as measured on the ratio-recorder

R = Reflectance of substrate/air interface

R_f = Reflectance of the evaporated film at the film/substrate interface

A = Absorption in the evaporated film

The transmittance measured on the dual-beam ratio recorder is

$$T_m = \frac{T_{fs}}{T_{ss}} . \qquad (10)$$

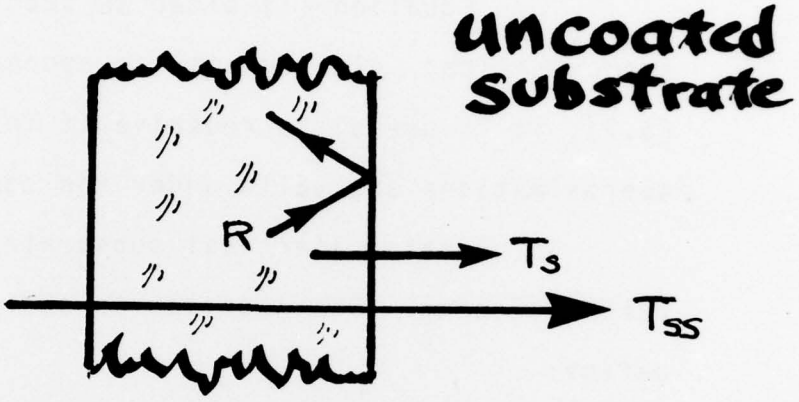

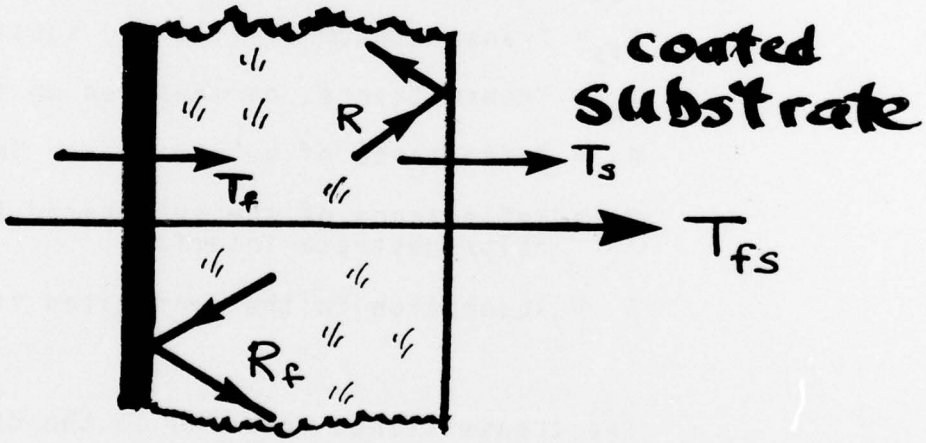

Fig 24

For a nonabsorbing substrate

$$T_{ss} = \frac{T_s^2}{(1 - R^2)} \tag{11}$$

$$T_{fs} = \frac{T_f\, T_s}{(1 - R_f R)} \quad . \tag{12}$$

Ergo:

$$T_m = \frac{T_f T_s/(1 - R_f R)}{T_s T_s/(1 - R^2)} \tag{13}$$

which reduces to

$$T_m = \frac{(1 + R)\, T_f}{(1 - R_f R)} \quad . \tag{14}$$

Using the identities

$$T_s = 1 - R, \tag{15}$$

$$T_f = 1 - R_f - A, \tag{16}$$

where A is the radiant absorption of the film, we find

$$T_f = \frac{T_m [1 + R(A - 1)]}{1 + R(1 - T_m)} \quad . \tag{17}$$

If $A << 1$, then Eq. (1) obtains:

$$T_f \cong \frac{T_m(1 - R)}{1 + R(1 - T_m)} \quad . \qquad (18)$$

5.2 The determination of the extinction coefficient $\underline{k}$ from the radiant absorption

The film of metric thickness $\underline{h}$ with optical constant $\hat{n} = \underline{n} - \underline{j}\,\underline{k}$ is deposited upon a substrate of index $\underline{n}$. The absorption $\underline{A}$ is defined in Eq. (17). When flux impinges upon the layer from the incident medium of index $\underline{n_o}$, the $\underline{A}/\underline{T}$ ratio is

$$\frac{A}{T} \cong \frac{k\left[(n^2 - n_s^2)S + \gamma(n^2 + n_s^2) + kn_s(2(C - 1) + \gamma^2)\right]}{2\,n_s(n^2 + k^2)} \qquad (19)$$

where γ is double the phase thickness of the layer

$$\gamma = 2\beta \qquad (20)$$

$C \equiv \cos\gamma$, and $S \equiv \sin\gamma$. is defined in Eq. (7). Equation (19) is precise in the expansion of the exponential function $\underline{\exp}\ (\underline{x})$ into terms of order $\underline{x}^2$.

It does not depend upon the refractive index $\underline{n_o}$ of the indicent medium, since $\underline{A}/\underline{T}$ is related to the "net flux ratio" and depends only upon the admittance of the medium on its emergent side. When the quadratic terms in $\underline{k}$ are ignored and the optical thickness is either a quarterwave or a halfwave, $\underline{A}/\underline{T}$ is directly proportional to the layer thickness.

6. References to the literature

1. P. Baumeister and O. Arnon: "Use of hafnium dioxide in multilayer dielectric reflectors for the near uv," Appl. Opt. 16, 439 (1977).

2. G. Hass, J.B. Ramsey, and R. Thun: "Optical Properties of various evaporated rare earth oxides and fluorides," J. Opt. Soc. Am. 49, 116 (1959).

3. E. Ritter: "Dielectric Film Materials for Optical Applications," in Physics of Thin Films, G. Hass, M. Francombe, and R. Hoffman, eds., (Academic Press, N.Y., 1975), Vol 8.

4. H. Bennett, A. Baer, R. Hughes, V. Rehn, J. Stanford: Ultraviolet components for high energy applications. US Naval Weapons Center Report NWC TP 6015 (March 1978).

5. H.E. Bennett and J.O. Porteus: "Relation between surface roughness and specular reflectance at normal incidence," J. Opt. Soc. Am. 51, 123 (1961).

6. H.E. Bennett and Jean M. Bennett: "Precision Measurements in Thin Film Optics," in Physics of Thin Films, G. Hass, M. Francombe, and R. Hoffman, eds. (Academic Press, N.Y., 1972), Vol 4.

7. J.M. Bennett, E.F. Ashley: "Calibration of instruments measureing reflectance of transmittance," Appl. Opt. 11, 1749 (1972).